Marine Geology 467 (2024) 107199

Contents lists available at ScienceDirect

Marine Geology

journal homepage: www.elsevier.com/locate/margo

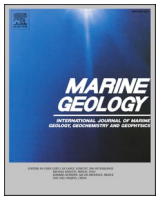

Research Article

A ~200-year relative sea-level reconstruction from the Wellington region (New Zealand) reveals insights into vertical land movement trends

Daniel J. King [a,b], Rewi M. Newnham [a,c,*], Andrew B.H. Rees [a], Kate J. Clark [d], Ed Garrett [b], W. Roland Gehrels [b], Timothy R. Naish [e], Richard H. Levy [e]

[a] School of Geography, Environment and Earth Sciences, Victoria University of Wellington, Kelburn Parade, Kelburn, Wellington 6012, New Zealand
[b] Department of Environment and Geography, University of York, Heslington, York YO10 5DD, United Kingdom
[c] School of Science in Society, Victoria University of Wellington, Kelburn Parade, Kelburn, Wellington 6012, New Zealand
[d] GNS Sciences, Ltd., 1 Fairway Drive, Avalon 5010, New Zealand
[e] Antarctic Research Centre, Victoria University of Wellington, New Zealand

ARTICLE INFO

Editor: Dr. Shu Gao

Keywords:
Saltmarsh
Foraminifera
Sea-level projections
Co-seismic uplift
Inter-seismic subsidence

ABSTRACT

The sea-level rise threat to New Zealand's coastal cities is regionally exacerbated due to spatially varying vertical land movement (VLM). At Wellington, the capital city, situated adjacent to a major active plate boundary, strong regional spatial and temporal variability of VLM is indicated by the relatively short (~25 year-long) continuous Global Navigation Satellite Systems (GNSS) network, but until now longer records of VLM have been lacking. Here, a ~ 200-year-long relative sea-level reconstruction is presented from Pāuatahanui salt marsh in the northern Wellington region. The foraminifera-based relative sea-level reconstruction indicates that ~1 ± 0.45 m of sudden uplift occurred during the 1855CE Mw 8.2 Wairarapa earthquake. Following this, Pāuatahanui has experienced a mean rate of relative sea-level rise (1855CE to present) of 1.5 ± 0.6 mm/yr, or 2.4 ± 0.8 mm/yr since the start of the twentieth century, consistent with ongoing subsidence in concert with climate-driven sea-level rise. Further acceleration to >3 mm/yr since the 1990s (with 4 mm/yr also possible if the full 95% confidence range is taken into consideration) is consistent with the globally documented acceleration in sea-level rise, although low model precision hampers confidence in this interpretation. This record is the first of its kind from a tectonically complex setting in New Zealand, shedding light on the effects of the historically significant 1855 earthquake, and fills a gap between millennial-scale and contemporary records of VLM with important implications for future sea-level projections in the region.

1. Introduction

As sea levels globally rise due to climate change, more settlements and habitats are at risk from flooding, aquifer salinization, and enhanced coastal erosion (e.g. Bird, 1996; Smith, 2010; Loáiciga et al., 2011; Takherani et al., 2020; Bell, 2021). Aotearoa/New Zealand's capital city of Wellington (Fig. 1) and its environments are at particular risk from enhanced relative sea-level rise because tectonically-driven vertical land movement (VLM) is modifying the trend of climatically-induced sea-level rise. Evaluating the contribution of local VLM to sea-level change projections is critical for understanding future risks and impacts around the region's coastlines (Tenzer and Gladkikh, 2014; King et al., 2020). International effort to quantify VLM in probabilistic projections of relative sea level has so far been restricted to locations of long tide-gauge records, where the non-climatic background related to VLM is extracted using a spatio-temporal approach (Kopp et al., 2014, 2015, 2017). Meanwhile, to increase spatial resolution, interferometric synthetic aperture radar (InSAR) velocity data calibrated by high-precision campaign and continuous Geographical Navigation Satellite System (GNSS) measurements are being used to build velocity fields of land deformation along the coastal strip (Poitevin et al., 2019; Biggs and Wright, 2020; Naish et al., 2022). In New Zealand and Wellington in particular, a key limitation of using these brief (maximum 20–25-years) geodetic time-series to approximate VLM in sea-level projections for the coming decades is the assumption that the short-term inter-seismic rates will continue to apply, and that the probability of rapid co-seismic

* Corresponding author at: School of Geography, Environment and Earth Sciences, Victoria University of Wellington, Kelburn Parade, Kelburn, Wellington 6012, New Zealand.
E-mail address: rewi.newnham@vuw.ac.nz (R.M. Newnham).

https://doi.org/10.1016/j.margeo.2023.107199
Received 21 July 2023; Received in revised form 23 November 2023; Accepted 4 December 2023
Available online 7 December 2023

changes in VLM, so far, cannot be incorporated. Furthermore, the recent satellite observations of VLM are revealing a high degree of spatial and temporal variability across the region. What addition VLM will make to relative sea-level change in the coming decades therefore remains highly uncertain.

Regional VLM complexity is explained by Wellington's tectonic setting adjacent to a major active plate boundary, where the underlying subduction interface has been shown to be elastically almost fully coupled (Fig. 1c; Wallace et al., 2012; Clark et al., 2019). A number of active faults cross the Wellington region, with individual fault rupture recurrence intervals ranging between 1145 years (Wellington fault) and 1230 years (Wairarapa fault) to many thousands of years. While dominantly strike-slip, the faults do have a reverse-vertical component, so while the recent (~20-year) VLM trend in the Wellington region is generally one of strong subsidence, on multi-century to millennial timescales, the net direction of VLM in the south and east of the Wellington region is upwards with rates averaging 0.5 mm/yr since the Last Interglacial maximum shoreline was formed (125,000 years ago) (King et al., 2020; Ryan et al., 2021; see Ninis et al., 2023 for further details). Moreover, Slow Slip Events (SSEs), which occur on the deep (>30 km) portion of the subduction interface, produce short-term changes in the rate of inter-seismic subsidence and can cause reversals (mm to multi-cm) in VLM direction on timescales ranging from weeks to years (Wallace and Beavan, 2010; Wallace et al., 2012; Wallace, 2020). The effect of SSEs is difficult to constrain due to limited continuous GNSS deployment across the Wellington region, but has been estimated to have offset approximately one third of the secular subsidence between 1996 and 2020 at the Kapiti GNSS site (Houlié and Stern, 2017; Denys et al., 2020). Significantly, to date there is no information available on the intermediate-term trends across multiple decades to centuries, to constrain the temporal variability of VLMs, and therefore, to evaluate the efficacy of short term geodetic estimates of VLM that may be used in future local sea-level projections for the coming decades (e.g. Naish et al., 2022).

Holocene sea-level records constructed from salt marsh sediments (e.g. Gehrels and Belknap, 1993; Horton, 1999; Southall et al., 2006;

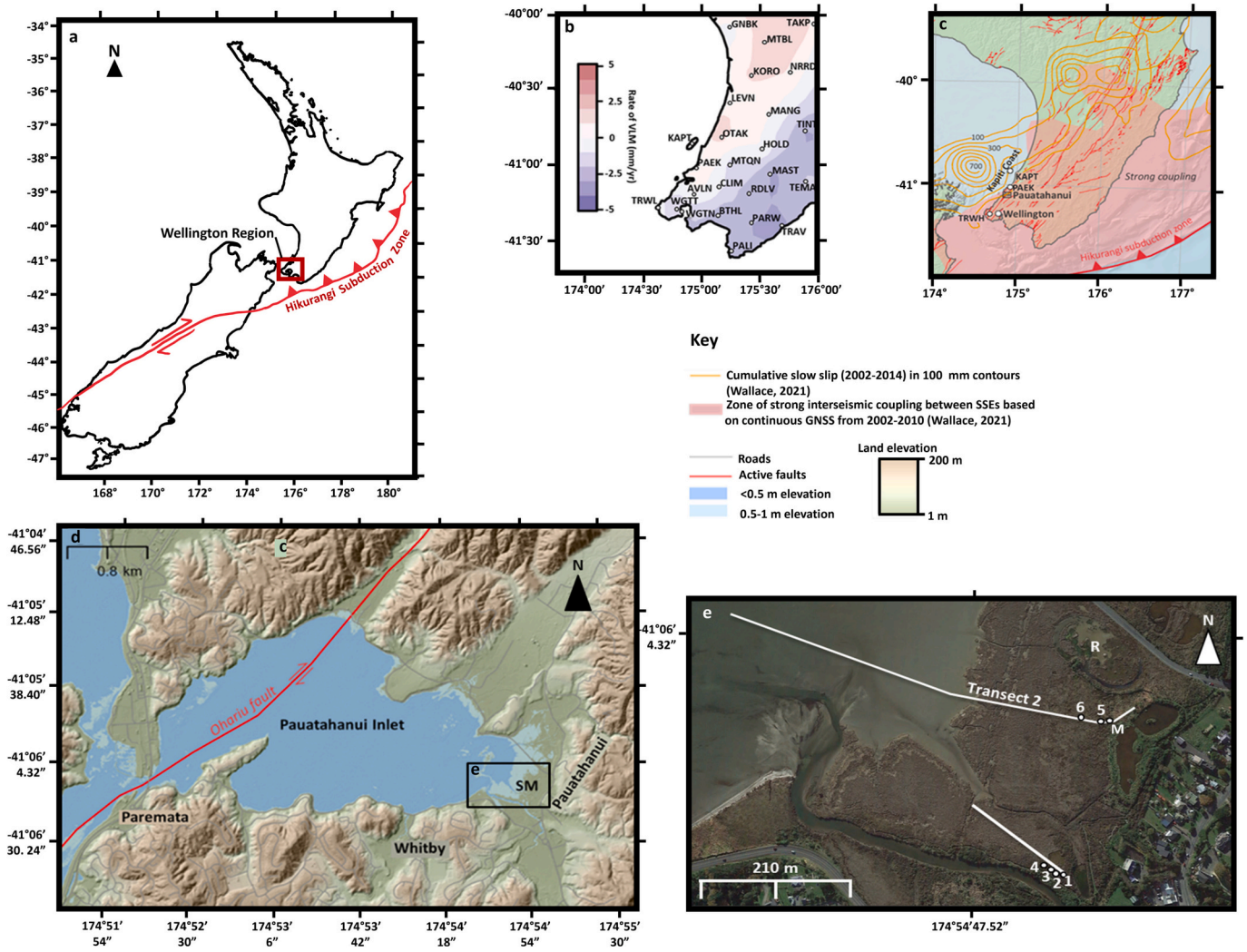

Fig. 1. a) Position of the Wellington Region in New Zealand, including the position of the Hikurangi Subduction Zone and associated plate boundary (positions drawn after Giba et al. (2013) and Fisher (2016)). **b)** Measured vertical land movement variability in the southern North Island, displaying the positions of GNSS stations. Modified after Houlié and Stern (2017). **c)** Tectonic setting of the Pāuatahanui Inlet. Active faults from the New Zealand Active Faults Database (https://data.gns.cri.nz/af/, accessed October 2021). Light pink shaded area shows the area of strong interseismic coupling on the Hikurangi subduction interface (adapted from Fig. 8b in Wallace, 2020). The orange contours show accumulated slow slip on the subduction interface from 2002 to 2014. PAEK = Paekakariki Hill GNSS site. The position of the Wellington tide gauge and WGTT GNSS stations are below the "Wellington" dot. **d)** Topography of the Pāuatahanui Inlet and location of the salt marsh (SM) study site. **e)** Positions of transects and cores at Pāuatahanui salt marsh. "R" represents the site of the former racetrack (Pāuatahanui Speedway). Numbers 1 to 6 represent the positions of the reconnaissance cores (Pau1 to Pau6, of which Pau2 was sampled for foraminifera), while M represents the position of the master core PauM1. (For interpretation of the references to colour in this figure legend, the reader is referred to the web version of this article.)

Gehrels et al., 2008; Barlow et al., 2013; Mills et al., 2013; Garrett et al., 2022; Williams et al., 2023), could provide insight into long-term RSL and the role of VLM rates, helping to evaluate the threat of future relative sea level change at locations of key interest. Here, we demonstrate the suitability of salt-marsh sediments in achieving this aim for the Wellington region. We present a new late Holocene sea-level reconstruction from foraminiferal assemblages preserved in salt marsh sediments at Pāuatahanui Inlet, approximately 30 km north of Wellington Central Business District (Fig. 1b). Our new record reveals the importance of VLM in modifying climate-driven sea-level change over the past ~200 years. In particular, it quantifies the local coastal uplift and relative sea level fall generated by the 1855CE Mw 8.2 Wairarapa Fault earthquake and then charts the subsequent sea level rise through to present. As the threat of VLM-enhanced relative sea-level rise is not unique to Wellington or New Zealand, this study is relevant to many other coastal communities and cities around the world that are experiencing VLM from a variety of tectonic and non-tectonic processes (e.g. Erkens et al., 2015; Nicholls et al., 2021; Restrepo-Ángel et al., 2021; Shirzaei et al., 2021; Stone, 2021).

2. Regional setting: Pāuatahanui inlet site background

2.1. Recent observations of regional vertical land movement

Pāuatahanui, lying both close to the SSE source region and atop the plate boundary (Fig. 1), has a history of recent and past long-term tectonically-driven VLM. The nearest GNSS site (Paekakariki Hill, ~9.4 km from the study site, station PAEK, Fig. 1b, c) records a mean vertical land movement trend of -1.7 ± 0.35 mm/yr subsidence since 2000, relative to the international reference frame ITRF2008 (Tenzer and Fadil, 2016), prior to the 2016 Kaikōura earthquake (see Supplementary Fig. 1). Subsidence from the site is notably less than the trend calculated for the Wellington tide gauge (-2.18 ± 0.17 mm/yr) by both Tenzer and Fadil (2016) and Denys et al. (2020). The PAEK record displays significant (~10–20 mm) periodic uplift during SSEs (GeoNet, 2020) that, depending on the timescale of examination, could negate the subsidence trend of -3.45 ± 0.12 mm/yr occurring between SSEs and other uplift events (Bell et al., 2018). Indeed, more recently the widely-reported subsidence (e.g. Tenzer and Fadil, 2016; Bell et al., 2018) at Paekakariki has been offset by a net uplift signal due to a combination of SSE and post-seismic uplift following the 2016 Kaikōura earthquake, which was observed across the entire Wellington region (Supplementary Fig. 1). As a result, the long-term VLM trend of Pāuatahanui Inlet is unclear on the basis of GNSS data alone, though it is noted that this trend may have recently returned to its pre-2016 rate.

InSAR data from a 3-km radius around Pāuatahanui indicate a mean subsidence rate of -2.2 ± 0.8 mm/yr from 2003 to 2011 (Hamling et al., 2022). NZ SeaRise (2022) used the InSAR-derived VLM estimates, which were calibrated using nearby GNSS data by Hamling et al. (2022), to generate model predictions for future relative sea-level rise rates for every 2 km around New Zealand's coast. For Pāuatahanui, the projections use the average rate of land subsidence across the 2 km area around the centre of the marsh (-2.32 mm/yr), with the assumption that the 8-year long 2003–2011 VLM trends will be continuous into the future. However, as is evident in Supplementary Fig. 1, there are complications from SSEs and earthquakes in the region. Whilst the VLM-adjusted NZSeaRise projections, based on the interseismic rate, includes SSEs, they are unable to include VLM resulting from future local and regional earthquakes.

2.2. Holocene palaeoseismicity and relative sea-level history

Beyond the recent observational record, Holocene investigations should provide insight into the role of VLM in local sea-level change. Previous proxy sea-level and palaeoseismic studies at Pāuatahanui Inlet have involved longer time scales and been at lower resolution than the work performed here (McFadgen, 1980, 2007, 2010; Eiby, 1990; Hayward et al., 2008; Wilson and Cochran, 2008; Clark et al., 2011; Gibb, 2012). Around 9 to 8 ka BP, the inlet, then a freshwater swampland, was inundated by the postglacial marine transgression (Blaschke et al., 2010; Gibb, 2012) and quickly developed into an extensive mudflat. The regional sea-level trend stabilised between 7.5 and 6 ka (Clement et al., 2016). However, Gibb (2012) reported positive and negative relative sea-level fluctuations on the order of several metres between 4.5 and 2.5 ka, indicating a period of significant tectonic unrest at the inlet. In a study of Ohariu Fault (Fig. 1d) movement, Litchfield et al. (2006) found evidence for one earthquake during this time interval, dated to 4810–3260 yrs. BP. Furthermore, Gibb (2012) noted that evidence for uplift was only observed on the west of the Ohariu Fault, with the magnitude of uplift decreasing northwards from 0.5 to 0.2 mm/yr.

Hayward et al. (2008) used foraminiferal data from several Holocene sediment cores in the inlet to infer a complex series of tectonic events, although these were not well constrained chronologically. Using a different suite of cores, Clark et al. (2011) reported no net tectonic deformation for Pāuatahanui Inlet since ~7000 cal yr BP. McFadgen (1980, 2007, 2010) interpreted a far more active palaeoseismic history for the inlet, on the basis of the elevations of beach ridges.

From this previous work, it can be concluded that for the past ~6.5 ka, Pāuatahanui Inlet has a somewhat ambiguous tectonic history, with possible subsidence events on the east of the Ohariu Fault, and potential evidence of uplift events on both sides of the Ohariu Fault, although primarily on the west. Coseismic uplift and interseismic subsidence appear to have largely cancelled each other out, resulting in an apparent long-term relative sea-level stability. This puts the area in contrast with the rest of the Wellington region, which has undergone a general net uplift over multi-millennial timescales (Beavan and Litchfield, 2012).

The distinctive sea-level and palaeoseismic history of the site when contrasted with the rest of the Wellington region highlights the need for local higher-resolution work at Pāuatahanui. It is important to understand whether the site is subjected to different rates of relative sea-level rise compared to central Wellington over multi-decadal timescales, and what implications this has for settlements in the northern Wellington region.

2.3. Impacts of the 1855 Wairarapa Earthquake on Pāuatahanui Inlet

The largest seismic event in Wellington in documented history is the 1855 CE Mw 8.2 Wairarapa earthquake (e.g. Grapes and Downes, 1997; Downes, 2005). Determining the effects of this earthquake on Te-Awarua-o-Porirua Harbour is important for understanding the role of tectonics in relative sea-level change in the Wellington region. However, the precise effects have proven to be difficult to resolve due to uncertainty in coastal uplift from estimates made at the time of the earthquake and from subsequent geomorphic interpretations. At Porirua Harbour, uplift estimates range from >2 m (Sheehan, 1987), through ~90–120 cm (Bennett, 1858; Adkin, 1921), ~60–70 cm (McFadgen, 1980), >30 cm (Lyell, 1856, in Grapes and Downes, 2010) to no uplift at all (Healy et al., 1980; Eiby, 1990).

The 1855 earthquake is widely considered to be the event that allowed the salt marsh at the head of the Pāuatahanui Inlet to form (Stephenson, 1986; Bellingham, 1998). Indeed, maps of the inlet show that the salt marsh was not present shortly before the 1855 earthquake (Park, 1841; McManaway and Gaz, 1852). A photograph from 1857 (available via NatureSpace, 2009) and a painting by Bradley (1865) (published in Sheehan, 1988) both show that the marsh was already forming shortly after the event and was well established within a decade. The 1855 age for the base of the marsh is also supported by historical observations of change to the high tide mark (Lyell, 1856, in Grapes and Downes, 2010; Bennett, 1858) and the documented raising of a locally popular diving spot now inside the marsh (Reilly, 2013). The weight of combined evidence strongly indicates that there was uplift at Pāuatahanui during the 1855 earthquake, although the magnitude of

uplift at the site is unresolved.

2.4. Land-use history

Human activity at Pāuatahanui salt marsh was likely to have generated usable chrono-stratigraphic markers, mostly as distinct changes recognisable in fossil pollen assemblages in the sedimentary record (Table 1). Following an extensive history of Māori occupation, the land surrounding Pāuatahanui was first colonised by European settlers in 1846 CE, with the adjacent town built between 1846 and 1848 (Reilly, 2013). The grass-dominated upper marsh was used for grazing and included a cattle yard (Adkin, 1917), from approximately the time of marsh formation (see Bradley, 1865, in Sheehan, 1988) until around 1980, when the site was purchased by a national conservation group, Forest and Bird (Conwell, 2010). During this agricultural phase, a motorcycle racetrack was established in the northern part of the marsh from 1938 until the mid-1950s (Reilly, 2013; McIsaacs, 2019a, 2019b), briefly re-opening in the mid-1970s (McIsaacs, 2019b). Of particular interest for chronological markers, extensive pine plantations were established in the region, and notably at nearby Whitby during the 1950s (Reilly, 2013). Aerial photography (Retrolens, 2021) shows a significant increase in forestry in and around the hills surrounding Pāuatahanui Inlet between 1947 and 1966, with relatively little expansion thereafter. More distal from the inlet, ~10 km northeast, pine plantations expanded from the 1970s to 1990s (Swales et al., 2005), so it would be expected that pine pollen deposition at the inlet would continue to rise across this interval as well (Blaschke et al., 2010). The establishment of a wildlife reserve at the marsh itself in 1984 (Reilly, 2013; Guardians of Pāuatahanui Inlet, 2021) led to the extensive removal of invasive plants and planting of native species. Ponds were built in the upper parts of the marsh to promote bird life in 1987 (Forest and Bird Pāuatahanui Reserve Committee, 2009). Despite these activities, there is little evidence of significant drainage or trenching/piling of sediment in the southern parts of the salt marsh. A consistent stratigraphy is observed across the upper marsh (section 4.2), supporting its use for sea-level reconstruction.

3. Materials and methods

3.1. Foraminifera as sea-level indicators

Salt-marsh foraminifera are an ideal microfossil group to use for sea-level reconstructions because they display tight vertical zonation relative to sea level in the modern environment (e.g. Scott and Medioli, 1980, 1986; Southall et al., 2006; Hayward et al., 1999a), particularly in the upper part of the marsh (e.g. Gehrels, 1994; Scott et al., 2001; Chen et al., 2020), where more precise reconstructions are usually obtained. Foraminifera are also very abundant in salt marshes, where they typically account for 24–75% of the meiofaunal biomass (Frail-Gauthier et al., 2019). Upper marsh foraminiferal assemblages are not prone to seasonal blooms and are compositionally highly consistent across a year (Hayward et al., 2014; Walker et al., 2020). The sedimentation rate in the uppermost salt marsh is strongly controlled by deposition during exceptionally high tides, and tends to closely track sea level, as the rise in relative sea level creates vertical accommodation space for sediment accumulation (e.g. Gehrels and Belknap, 1993; Swales et al., 2020; Gehrels and Kemp, 2021). The distribution of foraminiferal assemblages across a marsh relative to elevation can be quantified to generate transfer functions, defined as "empirically-derived equations for calculating quantitative estimates of past atmospheric and oceanic conditions from paleontological data" (Sachs et al., 1977). Transfer functions can be applied to build proxy reconstructions of past sea level using the fossil foraminiferal assemblages in sediment cores usually taken from upper marsh habitats (Kemp and Telford, 2015).

In this study, foraminifera (Fig. 2) were identified with reference to Hayward et al. (1999b), and occasionally other material. For example, *Polysaccammina ipohalina* was identified with reference to Scott (1976), and *Reophax* sp. using Hesemann (2020a, 2020b, 2020c). Morphotypes of *Trochammina inflata* (Montagu, 1808), which are sometimes treated as separate species (*Siphotrochammina lobata* (Saunders, 1957) and *Trochammina laevigata* (Cushman and Bronnimann, 1948a)) were common, and are here considered to represent intraspecific variability among *T. inflata*, in accordance with work by Javaux and Scott (2003), Barbosa and Scott (2006), Tobin et al. (2005), and Camacho et al. (2015), as well as with all prior New Zealand work (Hayward, pers. comm., 2020). The taxonomy of the genera *Trochamminita* (Cushman and Bronnimann, 1948b) and *Pseudotrochamminita* (King, 2021) are given in accordance with King (2021), and the taxonomy of the genus *Ammonia* (Brünnich, 1772) is given in accordance with Hayward et al. (2021).

Table 1
Key chrono-stratigraphic markers expected from land-use change and associated ages used in age-depth model (Fig. 9).

Marker or Land Use	Ages (AD years)	Horizon
1855 earthquake	1855 (earthquake)-1858 (colonisation complete before 1865) Input as: 1858 ± 3	Rapid colonisation of mudflat by salt marsh plants. Initiation of soil formation within 10 years
Use of upper marsh as pastureland	~1855–1980	Elevated pasture weeds in environment (*Taraxacum*, Asteraceae spp.), therefore in pollen assemblage
Acceleration in pine plantation	1950s–1960s (input as 1960 ± 9)	Expect rapid increase in pine pollen ~1960
End of pastureland usage	1980 (input as 1980 ± 5	Reclamation of upper marsh by true salt-marsh plants, decline in agricultural weeds (*Taraxacum*, Asteraceae spp.)
Building of ponds in the upper marsh	1987 (visible in core Pau2 only, not included in age model)	Possible shifts to fresher water foraminiferal assemblages

3.2. Fieldwork

Two transects were established across the north and south of the marsh at Pāuatahanui (Fig. 1d, e; Transect 1 in April 2019, Transect 2 in May and October 2019), with the transects being distal to one another to avoid spatial autocorrelation (e.g. see Telford and Birks, 2011; Crum et al., 2021). Along each transect, surface sediment samples were collected at 2- to 5-cm vertical intervals to provide for elevation changes of equivalent magnitude from the uppermost marsh to the lower mudflat. Elevation was measured using a Septentrio real-time kinematic (RTK) global positioning system (GPS) device. These data were then converted to the sea-level datum NZVD2016 (New Zealand Vertical Datum 2016) using a suite of nearby survey benchmarks, with a precision of +/− 2 cm indicated by the equipment. Sediment cores were collected using a gouge auger with a 6-cm wide barrel. Six test cores were collected to assess the site's stratigraphic consistency and two master cores were collected, one from either transect. Four duplicates were taken of each for chronology. Core sediments were logged and described using the sediment classification scheme of Troels-Smith (1955).

3.3. Laboratory processes

Samples of 5-ml volume, from surface and core sediments, were sieved between 500 and 63 μm to separate foraminifera from the sediment matrix (e.g. Southall et al., 2006; King, 2017; Chen et al., 2020) and were stored in 15-ml vials in deionised water and a squirt of denatured 99% ethanol. Samples were left for 24 h in 1 g/L rose Bengal stain immediately after washing (as per Murray, 1991). This process stains cell cytoplasm and enables identification of live foraminifera,

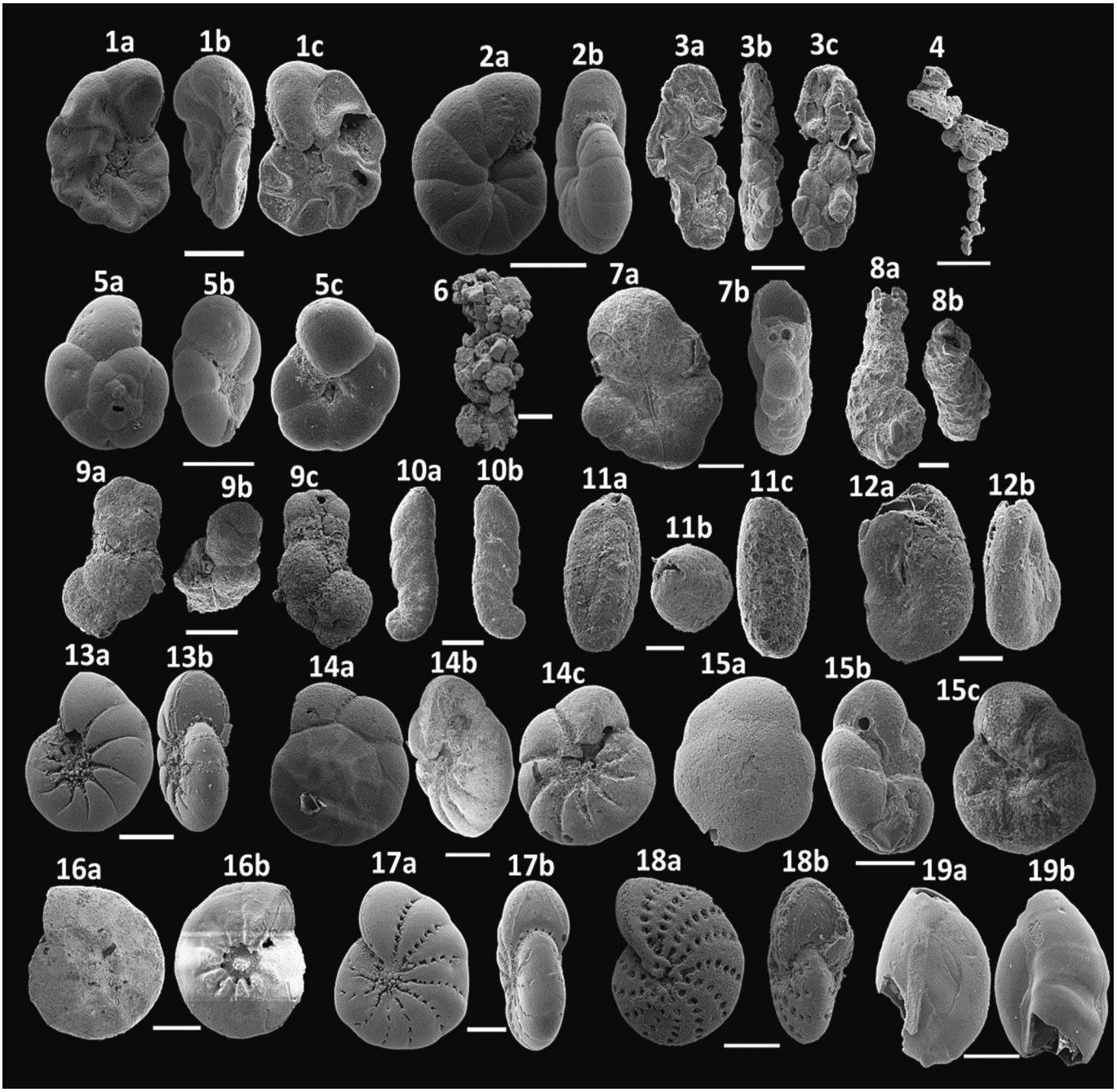

Fig. 2. Foraminiferal species observed along the two studied transects: 1. *Entzia macrescens* (single-aperture morphotype). Scale bar: 200 μm. a) ventral view b) apertural view c) dorsal view. 2. *Haplophragmoides wilberti*. Scale bar: 200 μm, a) anticlockwise-coiling view b) apertural view. 3. *Pseudotrochamminita malcolmi*. Scale bar: 100 μm, a) side view b) apertural view c) side view. 4. *Polysaccammina ipohalina*. Scale bar: 200 μm, apertural view. 5. *Trochammina inflata*. Scale bar: 200 μm, a) dorsal view b) apertural view c) ventral view. 6. *Reophax* sp. Scale bar: 200 μm, side view. 7. *Trochamminita salsa*. Scale bar: 100 μm, a) side view b) apertural view. 8. *Ammobaculites exiguus*. Scale bar: 100 μm, a) side view b) apertural view. 9. *Trochamminita irregularis*. Scale bar: 200 μm, a) side view b) ventral view c) apertural view. 10. *Ammotium fragile*. Scale bar: 100 μm, a) side view b) side view. 11. *Miliammina fusca*. Scale bar: 50 μm, a) dorsal view b) apertural view c) ventral view. 12. *Glomospira fijiensis*. Scale bar: 50 μm, a) side view c) dorsal view (aperture not visible, compressed against spiral side)0.13. *Haynesina depressula*. Scale bar: 100 μm, a) side view b) apertural view. 14. *Ammonia aoteana*. Scale bar: 100 μm, a) dorsal view b) apertural view c) ventral view. 15. *Ammonia veneta*, Scale bar: 50 μm, a) dorsal view b) apertual view c) ventral view. 16. *Ammonia* sp. Scale bar: 100 μm, a) dorsal view b) ventral view. 17. *Cribroelphidium excavatum*. Scale bar: 100 μm, a) side view b) apertural view. 18. *Elphidium maorium*. Scale bar: 100 μm, a) side view b) apertural view. 19. *Quinqueloculina* sp. Scale bar: 100 μm a) dorsal view b) ventral view. Specimens 4 from Aramoana salt marsh, Dunedin, 13 from Catalina Bay, Auckland, 18 and 19 from Rangitoto Island, Auckland. All other imaged specimens from Pāuatahanui).

though it is noted that some studies have found cytoplasm to persist well beyond death (e.g. Bernhard et al., 2006). To eliminate taphonomic and seasonal biases and thereby provide for surface samples more analogous to fossil assemblages (e.g. Murray, 1991, 2000), only unstained (definitively dead) foraminifera were picked and counted. Samples were picked wet to avoid the clumping of organic matter and damage to tests upon drying.

Although Kemp et al. (2020) recommend that no samples with <50 foraminifera should be used to develop the transfer functions, this threshold was not achievable for the surface samples covering the

uppermost 8 cm of the study area. Excluding this large subsample would bias the transfer function and fail to encapsulate the uppermost marsh environment. As a result, a compromise minimum count of 40 was considered acceptable, as has been applied in other low-diversity salt-marsh environments. Kemp et al. (2020) found that training sets restricted to >50 foraminifera only showed marginal improvements in R^2 and RMSEP compared with sample sets containing only >40 foraminifera. Recent work by Garrett et al. (2022) generated a reliable reconstruction using an even lower minimum count (30 foraminifera). High-abundance samples were split to enable a more manageable workload using a wet splitter, as described in Scott and Hermelin (1993).

3.4. Chronology

Core chronology for both the master core, PauM1, and its adjacent duplicates was based on ^{210}Pb dating, constrained by historical events identified through palynological and stratigraphic analysis. The lack of clear stratigraphic horizons that could be tied to historical events prior to 1855, combined with the lack of reliable organic fractions for radiocarbon dating in the pre-salt-marsh sediments, meant that it was only possible to generate an accurate chronology for the post-1855 sequence.

Pollen samples of 1 cm^3 were collected at each centimetre interval down-core for comparison with historical vegetation change records (Table 1). Pollen counts were 250 dryland pollen per sample for all samples above 21.5 cm, with some gaps due to low-yield samples. The lower sand-rich sediment contained insufficient pollen for reliable counts. In accordance with New Zealand palynology convention (e.g. Newnham et al., 1995), pollen percentages were calculated with reference to the 'dryland' pollen sum (dlp) of trees(t), shrubs(s) and herbs (h), including exotics (i.e. dlp = Σt + Σs + Σh + Σe). For taxa from each of the non-dryland categories, i.e., salt marsh (m), freshwater (w) and ferns/tree ferns (f), the percentages were calculated from a sum comprising all dryland pollen plus all pollen from that particular category.

Radiogenic lead ($^{21\circ}$Pb) is a part of the decay series of ^{238}U, and its presence in sediments has two main sources: supported $^{21\circ}$Pb (which forms through decay in the sediments) and unsupported $^{21\circ}$Pb (atmospheric fallout) (e.g. Appleby, 1998; Andersen, 2017; Cook et al., 2018; Bruel and Sabatier, 2020). To measure the activity of $^{21\circ}$Pb, sediment samples were collected (at a minimum of 5 g) down-core, and their volumes measured using water displacement. Samples were then dried and weighed to measure their density. The samples were sent to the gamma-spectrometry lab at the Institute of Environmental Science and Research (ESR), Christchurch. Because of the 22.5-year half-life of $^{21\circ}$Pb, the technique is able to derive relatively precise chronologies over the past century, and potentially over the past 150 years (Appleby, 1998; Andersen, 2017), making it ideal for the timescale of this study.

To derive an age-depth model, the Bayesian $^{21\circ}$Pb age model rPlum (Aquino-López et al., 2018; Blaauw et al., 2021) was employed. rPlum enables the inclusion of secondary chronological data (such as the aforementioned chronomarkers and pollen data), models uncertainties, and does not rely on using the lowermost core samples to represent $^{21\circ}$Pb "background". As a result, rPlum can extend the chronology further back in time than the other $^{21\circ}$Pb models (Aquino-López et al., 2018).

3.5. Statistical analyses

Sea-level transfer functions were applied to the fossil foraminiferal data using the software RStudio Desktop, utilising R version 4.2.1 (R Core Team, 2022). Transfer functions were generated and tested using the packages vegan (Oksanen et al., 2019) and rioja (Juggins, 2019), updated versions of the packages recommended for use in sea-level reconstruction by Kemp and Telford (2015). The software includes the following transfer function models: Maximum Likelihood by Response Curves (MLRC), Modern Analogue Technique (MAT), Partial Least Squares (PLS), Weighted Averaging (WA), locally weighted-weighted averaging (LW-WA) and Weighted Averaging Partial Least Squares (WA-PLS). The statistical background underpinning these models and their differences are outlined by Kemp and Telford (2015). Their applicability for each site was tested using leave-one-out cross-validation, a technique by which each sample is removed from the training set, and the remaining samples are used by the model to reconstruct the elevation of the removed sample (Kemp and Telford, 2015). Under this technique, the relationship between observed and predicted values is used to evaluate transfer function suitability, on the basis of higher R^2 and lower RMSEP values. Model evaluation also uses trends in the cross-validation plot which may show significant zones of over- and under-prediction and trends/unevenness in residual errors, defined as the predicted value minus the observed (Eggermont et al., 2006). Because RMSEP is generally 10–15% of a site's tidal range, sites with smaller tidal ranges typically result in more precise transfer function models (Barlow et al., 2013; Williams et al., 2021).

To determine whether species response is unimodal or linear (and thus which models are most appropriate), detrended canonical correspondence analysis (DCCA) was applied to each training set using the software CANOCO (ter Braak and Verdonschot, 1995; Šmilauer and Lepš, 2014). Examples of unimodal models are MLRC, WA, LW-WA, and WA-PLS, while an example of a linear model is PLS. Under this analysis, standard deviation gradient lengths exceeding 2 SD units indicate unimodal species responses, while lengths below 2 indicate linear species responses (e.g. Birks, 1995; Massey et al., 2006; Mills et al., 2013). Regional transfer functions were not attempted, as the highest occurrence of foraminifera was not reached by either transect, meaning that the tidal range for the site could not be reliably determined (see Wright et al., 2011), and the data could not be assigned to a standardised water level index value. As greater precision can often be derived from transfer functions generated only using marsh training sets that exclude mudflat samples (Barlow et al. (2013), models were assessed both with and without mudflat sediments. Mudflat-excluding models were not used to assess the amount of uplift during the 1855 earthquake, because they cannot be applied to non-salt marsh sediments.

Change-point linear regression (CPLR) (Cahill et al., 2015; Cahill, 2021) was used to test for the timings and statistical significance of accelerations and/or decelerations in the reconstructed rates of sea level change (Supplementary Fig. 1). CPLR forces the data into linear sections, avoiding discontinuity, and uses Gibbs' sampling techniques to locate the timing of changes in trends (Carlin et al., 1992; Cahill et al., 2015). CPLR was run using the packages tidyverse (Wickham, 2021), rjags (Plummer et al., 2021), and R2jags (Su and Yajima, 2021).

4. Results

4.1. Modern training sets from surface transects

Surface Transect 1, in the southern part of the marsh, extends 168.5 m horizontally across several distinct vegetation zones and the upper tidal flat and covers a vertical range of 0.94 m above mean sea level (amsl) to 0.05 m amsl (Figs. 1d, 3).

The dead foraminiferal assemblages of the uppermost marsh samples (vegetation zone dominated by shrubs and grasses) are dominated by up to 100% *Entzia macrescens,* all belonging to the single-aperture morphotype often considered indicative of low-salinity conditions (Scott and Medioli, 1980; cf. Gehrels and van de Plassche, 1999). The mid-marsh zone, vegetated by *Selliera radicans* and *Salicornia quinqueflora,* is dominated by *Trochammina inflata*, with the low marsh (*Juncus kraussii* vegetation zone) being dominated by the species *Haplophragmoides wilberti*. The upper tidal flat has an assemblage dominated by *Ammobaculites exiguus* and a variety of similar species within the family Elphidiinae (including *Cribroelphidium excavatum, Cribroelphidium clavatum, Elphidium maorium* among others), and within the genus *Ammonia*

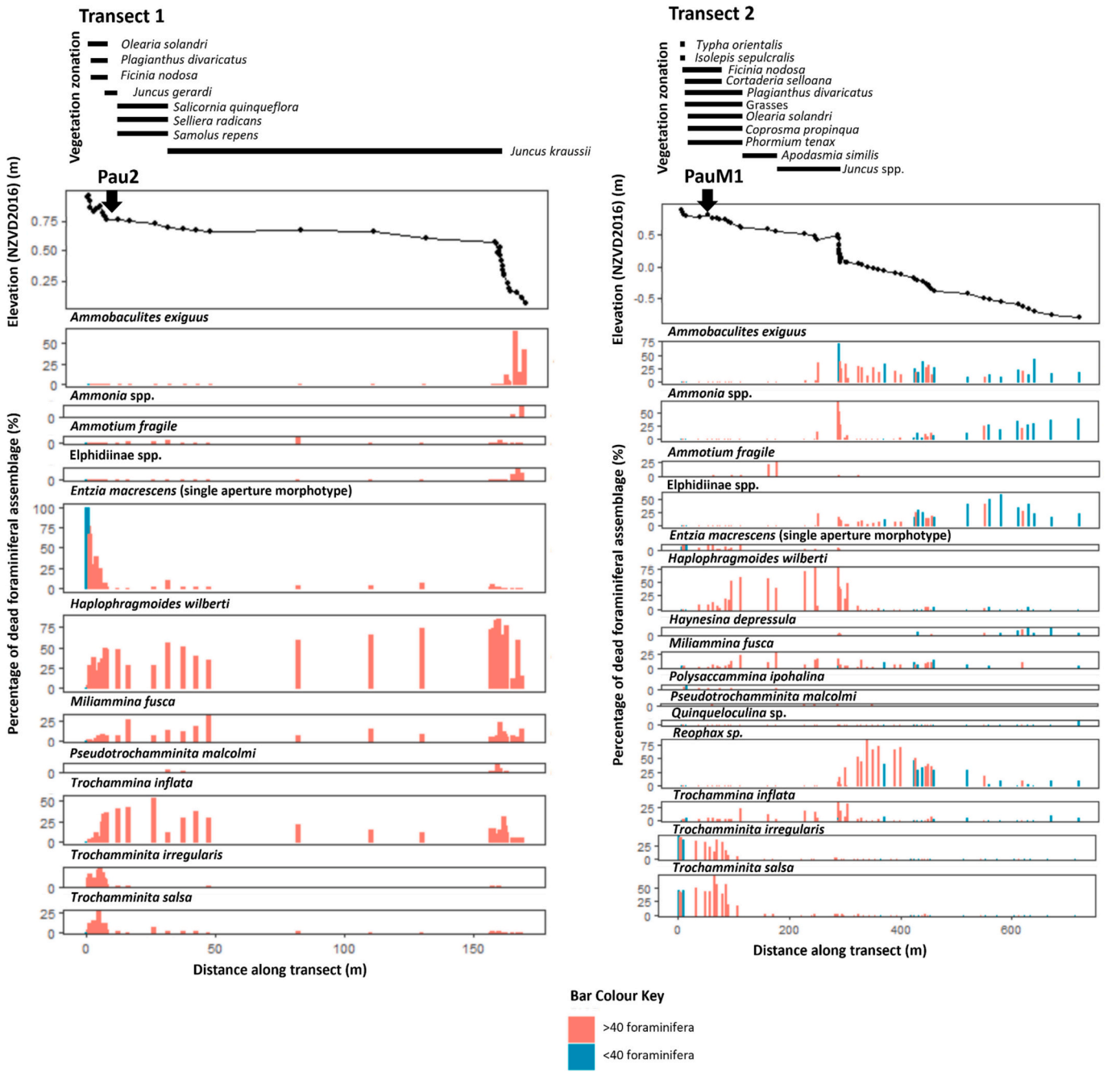

Fig. 3. Vertical profile of Transects 1 (left) and 2 (right), plotted over distance, displaying the change in vegetation and dead foraminiferal assemblage.

(*A. aoteana* and *A.veneta)*. Many *Ammonia* specimens could not confidently be assigned to either New Zealand species due to high intraspecific variation. This study is the first to observe both *A. veneta* and *Glomospira fijiensis* in New Zealand south of Auckland (Hayward et al., 1999b). *Miliammina fusca* is found in low abundances across the entire vertical range of the transect.

Surface Transect 2 in the north of the marsh (Fig. 1e), spans 728 m and covers an elevational range of between 0.88 m above msl and 0.82 m below msl (Fig. 3). The high-marsh (vegetation dominated by *Typha orientalis*, grasses, pampas grass, shrubs, and sedges) foraminiferal assemblage differs markedly from Transect 1, despite covering much of the same elevational gradient. For example, in Transect 2, the high marsh is dominated by *Trochamminita* spp. (*T. salsa* and *T. irregularis* (sensu Callard et al., 2011)), with *E. macrescens* never comprising >20% of the foraminiferal assemblage. As is clear when surface assemblages from the two transects are plotted together against elevation (Fig. 4), the foraminiferal assemblage distribution of the remainder of the transect is similar to that of Transect 1, with *H. wilberti* dominating the mid (vegetated by *Apodasmia similis*) to low (vegetated by *Juncus* spp.) marsh, before declining in abundance in the upper tidal flat. As with transect 1, *M. fusca* is observed in low abundances at all elevations, from the top of the transect to its base. Transect 2 also shows a clear succession in foraminifera across the tidal flat, with *Ammobaculites exiguus* common throughout; *Ammonia* spp. displaying a bimodal distribution, dominating both the marsh-tidal flat boundary and being abundant again in the low tidal-flat; and Elphidiinae spp. being most abundant in the mid-tidal flat, around 550 m distance. The upper tidal flat in Transect 2 is dominated by an unidentified, potentially undescribed, *Reophax* species (Fig. 2). *Polysaccammina ipohalina* was present in the upper marsh of transect 2, but absent entirely from transect 1.

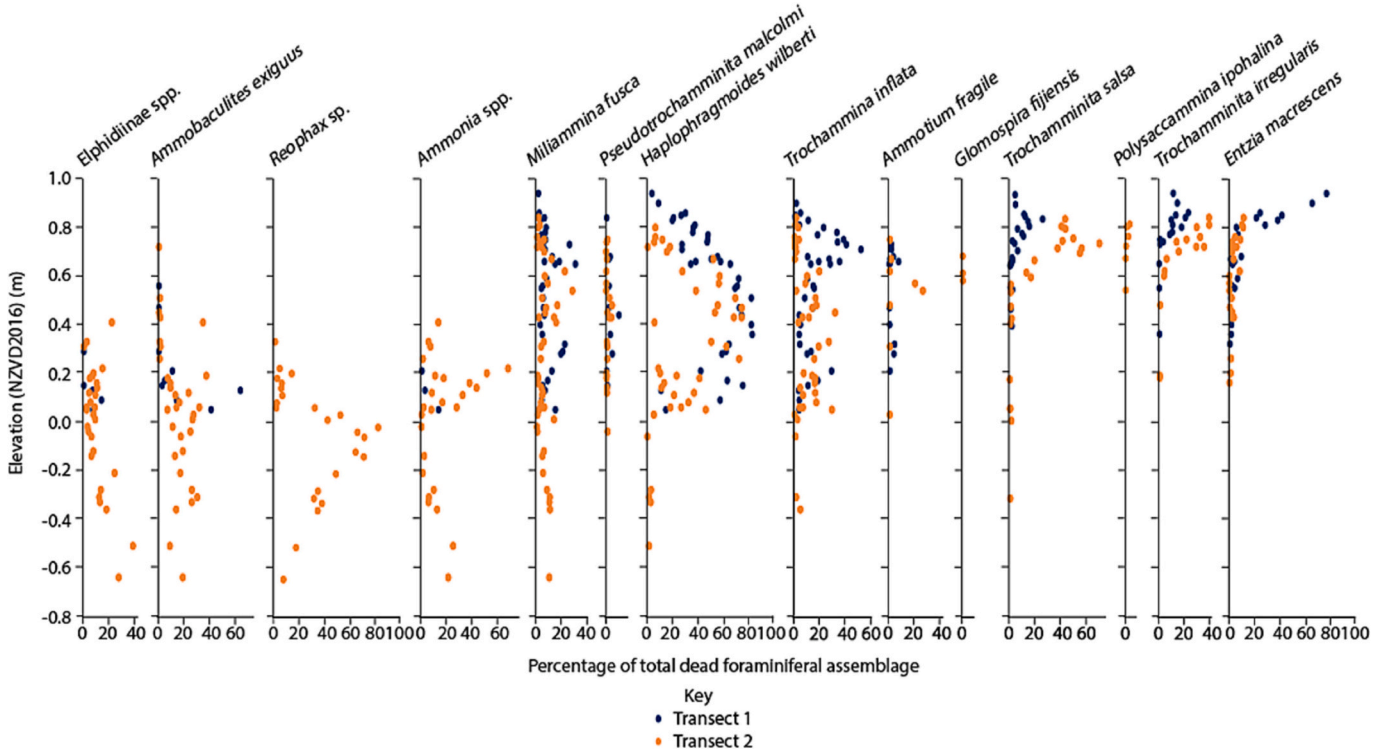

Fig. 4. Percentage of foraminiferal taxa for all surface samples containing >40 specimens, plotted against elevation in order of WA-modelled species optima.

4.2. Stratigraphy and biostratigraphy

Across the marsh, the lowermost layer encountered is a blue-grey, fine sandy silt, which is sharply overlain by medium to coarse shelly sand predominantly containing the bivalve *Austrovenus stutchburyi*. The shelly sand is itself sharply overlain by a 16 to 23 cm-thick peat or

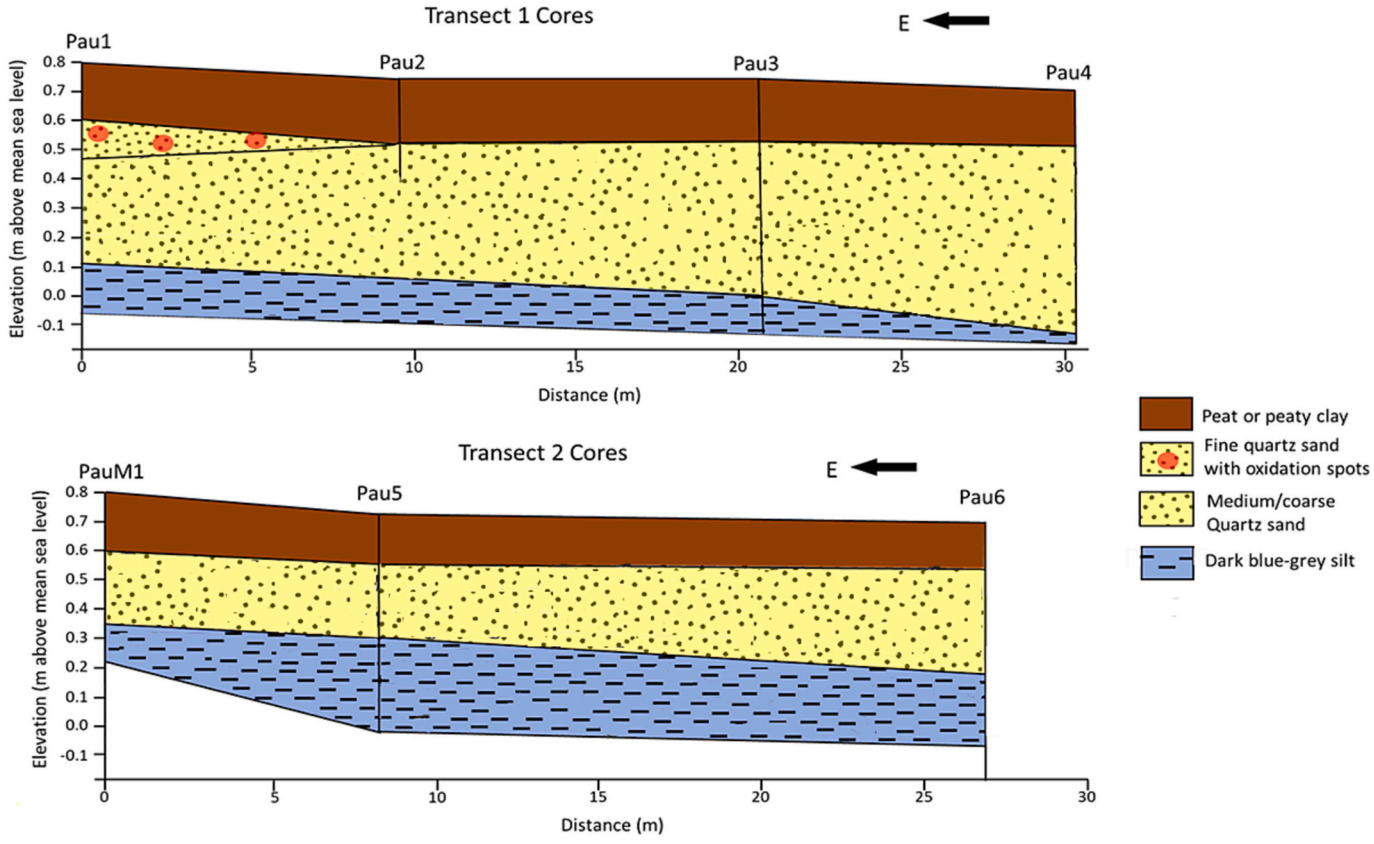

Fig. 5. Simplified stratigraphy of sediment cores taken from across Pāuatahanui salt marsh (positions in Fig. 1d).

organic-rich clay sequence indicative of salt marsh sedimentation. This stratigraphic sequence has been replicated in six test cores from across the upper marsh (Figs. 1d, 5, detailed logs presented in supplementary material) and in a total of 21 cores from across the entire marsh during another investigation (Albot, pers. comm., 2022).

The master core PauM1 (at 0.80 m elevation) and the shorter, reconnaissance core Pau2 (at 0.75 m elevation) were picked for foraminifera (Fig. 6). In both cores, the basal shelly sands, representing tidal mudflat environments, are dominated by *Ammonia* spp. with a sharp biofacies transition to *Rheophax* sp. towards the top of the lithofacies. Despite a clear stratigraphic change down-core, the shift from shelly medium sand to less fossiliferous fine-sandy silt is not associated with a noticeable foraminiferal assemblage change in core PauM1. Similarly, the abrupt up-core shift from *Ammonia*-dominated to *Reophax*-dominated foraminiferal assemblages is also not associated with a visible change in sedimentology. In both cores, the uppermost ~21 cm of brown peats or organic-rich clay are dominated by upper-marsh assemblages (Trochamminita spp. in PauM1 and *Entzia macrescens* in Pau2, with the upper 5 cm of Pau2 dominated by *Trochammina inflata*).

4.3. Chronology

On the basis of the local historical record and tectonic context, the abrupt transition from sandy to peaty sediments at 21 cm depth down-core can be confidently attributed to the 1855 CE earthquake. This is supported by international work which has shown how sharp, laterally consistent emergent transitions from silty/sandy sediment into marsh peats can be due to earthquakes (e.g. Nelson et al., 1996; Shennan et al., 2016). Historic accounts of coseismic uplift are consistent with the rapid uplift implied by the shift in foraminiferal assemblages, and the shift in sediment type (from sand to peat) matches what would be expected at the onset of salt-marsh formation. An independent radiometric estimate of the date of this horizon was unachievable due to a lack of radiocarbon dateable material and the fact that rPlum was unable to model chronology down to this depth using ^{210}Pb alone. Nevertheless, the pollen assemblages (Fig. 7a) in the lowermost marsh peats (from 21 cm depth) are consistent with a mid-nineteenth century age, with the native tree rimu (*Dacrydium cupressinum*) dominant and low but gradually increasing levels of pine (*Pinus* sp.), which was introduced to the region by the earliest European settlers from the mid-nineteenth century. The balance between pine and rimu progressively changes, with pine undergoing a notable up-core increase in abundance, particularly between 9 and 10 cm depth, due to expansion of pine plantations in the region. This increase is likely associated with the 1950s–1960s planting of >79,000 pine trees over 500 acres nearby (Reilly, 2013), while *D. cupressinum* gradually declines in abundance up-core due to progressive culling of native vegetation, as also observed by Swales et al. (2005). An abrupt decline in *Taraxacum* spp., a ruderal herb associated with agriculture, and other Asteraceae above 6.5 cm depth is consistent with a decline in grazing (see Li et al., 2008), likely associated with the end of the use of the upper marsh for pastureland in 1980 after its purchase by Forest and Bird conservation group (Conwell, 2010).

Down-core sampling for ^{210}Pb at 1-cm (first 10 cm) and 2-cm (below 10 cm) intervals was integrated with these stratigraphic horizons. The abrupt 21-cm-depth stratigraphic transition is input to the age model (Fig. 7b) as 1858 CE ± 3 years, allowing for incipient marsh habitat to take several years to establish. The 9.5 cm increase in pine is input as 1960 CE ± 9 years (to allow the initial 1950s plantation seedlings ~1 decade to mature and account for a subsequent rise in pine pollen. This age is based on the detailed local history presented by Reilly (2013), historical aerial photography (Retrolens, 2021) and a sharp drop in ^{137}Cs between 10.5 and 8.5 cm, consistent with ~1965 peak fallout in New Zealand - see Garrett et al. (2022) (cf. e.g. Andersen, 2017; Corbett and Walsh, 2015; Drexler et al., 2018). The 6.5 cm drop in *Taraxacum* spp. abundance, signalling the curtailment of agriculture and commencement of local conservation efforts, is input as 1980 CE ± 5.

4.4. Transfer function development

Following Kemp and Telford (2015), we developed one transfer function model using all surface samples (79 samples), including those from the tidal flat, and another using just the vegetated marsh samples (53 samples). The marsh-specific transfer function included samples immediately underlying the lowermost marsh sample (0.20 m (NZVD2016)). Minimum, maximum, and average foraminifera counts are 40, 356, and 165, respectively, with standard deviation of 81.9.

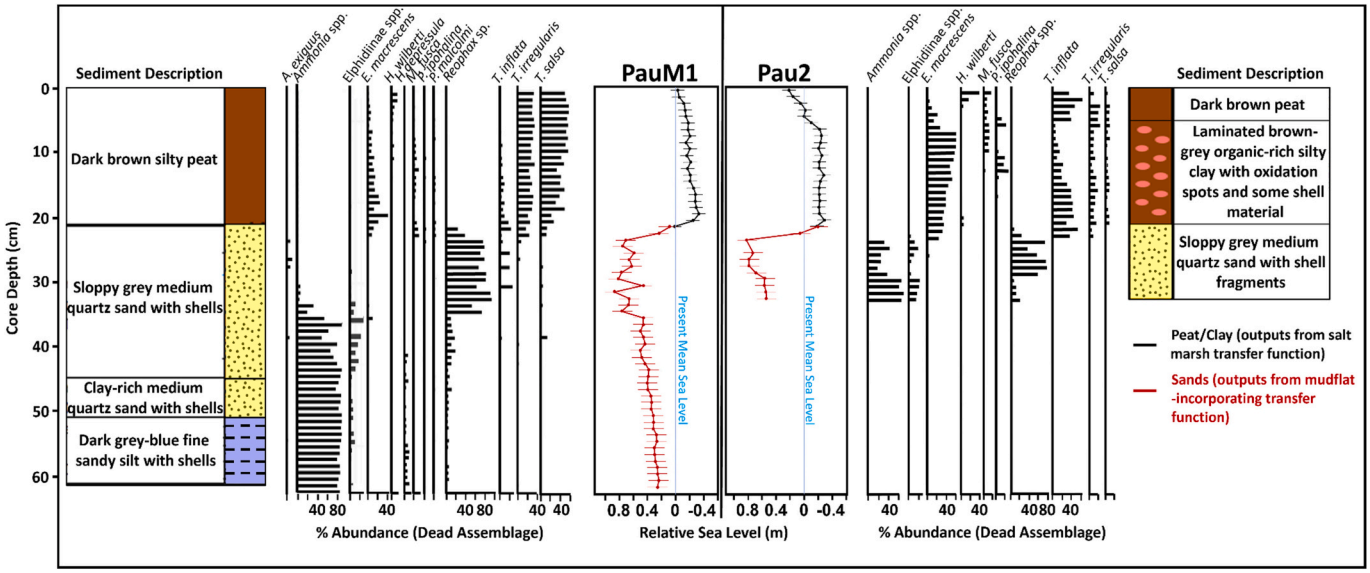

Fig. 6. Down-core foraminiferal assemblages and relative sea-level reconstructions for cores PauM1 (left) and Pau2 (right), plotted against simplified stratigraphic logs and core depth. Note that the "Pau2 sand" and "PauM1 sand" reconstructions are considered less reliable due to biases within the whole training-set transfer-function, as discussed in section 4.4. On the basis of modern surface sedimentary composition and foraminiferal assemblage, peats and organic-rich clays are interpreted to represent salt marsh sediments, while shelly sands are interpreted to represent mudflats. Sandy silts are also interpreted to represent a mudflat environment on the basis of their foraminifera.

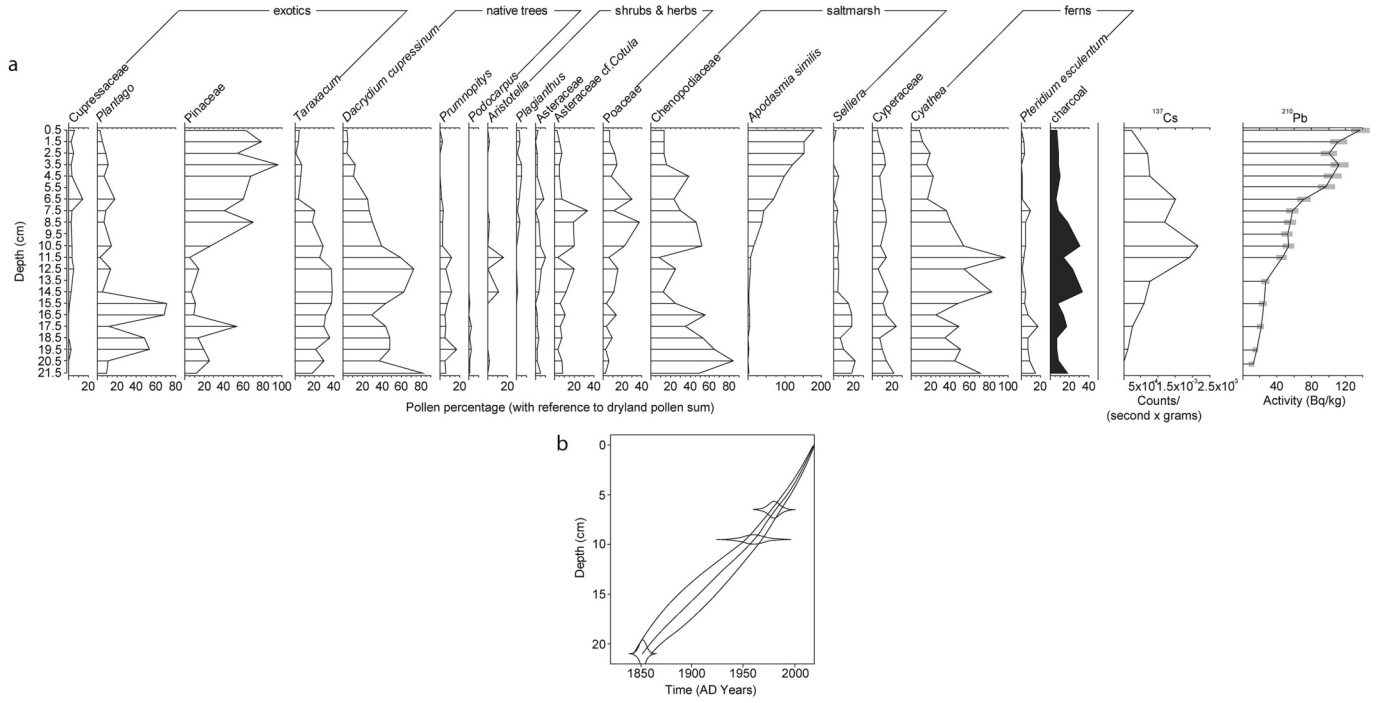

Fig. 7. a) Down-core pollen and charcoal assemblages, and radioisotope activity profile from core PauM1. **b)** Bayesian rPlum-derived age model for sediment core PauM1. Horizon a reflects the 1855 earthquake (calibrated at 1858 ± 3 years), b represents the ~1960 pine pollen increase (supported as-mentioned in text by unincorporated ^{137}Cs data, which would be expected to have a broader uncertainty due to the absence of a ^{137}Cs sample at 8.5 cm depth), and c represents the ~1980 *Taraxacum* drop. Blue squares represent ^{210}Pb in Bq/kg. The top panels show model variation with progressive iterations, and prior (green lines) and posterior (grey shaded zones) distributions for accumulation rate, memory, supply of ^{210}Pb and supported ^{210}Pb. (For interpretation of the references to colour in this figure legend, the reader is referred to the web version of this article.)

DCCA gives a gradient length of 4.071, indicating unimodal distribution (Birks, 1998; Wright et al., 2011), and estimates that 27.3% of variability within the foraminiferal assemblage is attributable to elevation. For the marsh-only training set, DCCA reveals a gradient length of 2.152, narrowly indicating a unimodal species distribution, with 20.1% of the assemblage variation being explained by elevation.

The performance for each tested model that assumes unimodal distribution is outlined in Table 2, with all models other than LW-WA (full training set) and 2-component WA-PLS (marsh-only training set) displaying notable biases in their residual predicted sample elevations, or (in the case of MLRC) creating spurious, more erratic predictions.

For the whole-assemblage model, classical LW-WA was chosen due to its more accurate estimation of the top of core PauM1 than the inverse model, and higher precision and R^2 than all non-LW-WA models, with the exception of MLRC, which displayed erratic features in its reconstruction. The selected model shows overall good performance across the marsh and upper mudflat, but tends to underpredict elevations of samples at around 0 m NZVD2016 and overpredict elevations below this. Pre-1855 reconstructions using this model are therefore treated with caution. For the marsh-only reconstruction, the 2-component WA-PLS model was selected as it also performs well, with no evidence in residual predicted heights for a systematic bias within the model above 0.45 m (Fig. 8).

Table 2
Transfer function performance for the full and marsh-limited training sets, following cross-validation. Asterisks denote the chosen models.

	Full training set		Marsh-limited training set	
Technique	**RMSEP (cm)**	R^2	**RMSEP (cm)**	R^2
LW-WA (inverse)	13.07	0.88	10.44	0.72
LW-WA (classical)	13.67	0.88	13.41	0.70
WA (inverse)	14.29	0.85	10.11	0.73
WA (classical)	15.29	0.85	13.92	0.70
WA-PLS (2 component)	14.21	0.85	9.64	0.76
WA-PLS (3 component)	14.18	0.85	8.13	0.83
MLRC	10.93	0.91	10.30	0.73
MAT (5 ANALOGUES)	11.50	0.90	9.44	0.78

4.5. *Model outputs and sea-level reconstruction*

Transfer function outputs (of both models) for the two cores show very similar sea-level reconstructions, although the uppermost top of core Pau2 fails to accurately reconstruct the core top within error (Fig. 6), possibly due to the impact of an abrupt up-core salinity shift associated with the building of the adjacent pond, while the reconstruction from core PauM1 underestimates the elevation of the core top by only 2.5 cm (marsh-limited model). Most emphasis is therefore placed on core PauM1 in the discussion of data.

Although there is no chronological data for the pre-1855 sands, and model performance renders this part of the record less trustworthy (Fig. 8), both reconstructions indicate a gradual but sustained apparent relative sea-level rise, and no earthquake-indicative abrupt changes in palaeoelevation below 34.5 cm depth. A period of potential vertical instability may be indicated by an abrupt shift in foraminiferal assemblages, prior to the 1855 earthquake, between 33 and 37 cm (Fig. 6), from *Ammonia*-dominated to *Reophax*-dominated. Since *Ammonia* displays a bimodal distribution in the site's upper and low mudflat environments, it is unclear exactly what sense of movement (uplift or subsidence) is indicated by this shift, with possible subsidence indicated by the transfer function outputs, though of an amount less than the total error of the transfer function outputs (Fig. 6). As climate-driven (i.e. not accounting for VLM) sea level reconstructions from New Zealand consistently show sea level to be falling or stable during the late Holocene (Clement et al., 2016), these observations from the sands underlying the marsh sediment are consistent with modern observations for long-term subsidence at the site, although we cannot say at what rate.

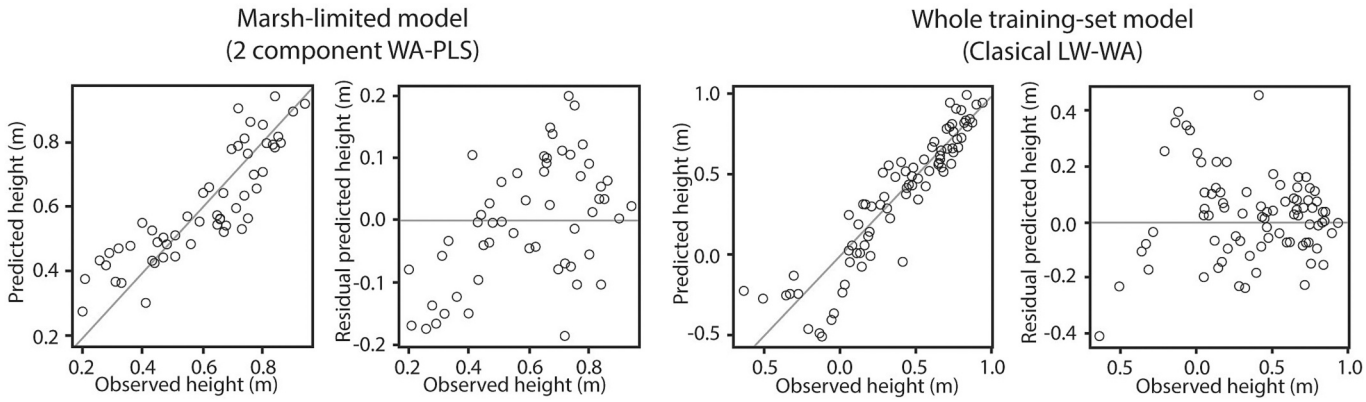

Fig. 8. Performance of the two selected models, displaying the relationships between predicted and observed elevation and residual predicted elevations for the two-component WA-PLS model (left) and classical LW-WA (right). In both cases, lower elevations are poorly estimated.

5. Discussion

5.1. Uplift during the 1855 earthquake

Both cores record marked uplift from the 1855 earthquake estimated as ~1.00 ± 0.45 m at 21 cm depth down-core (Fig. 6). This ~1 m uplift is replicated by all models presented in Table 2. The error range encompasses a previous uplift estimate of ~60–70 cm by McFadgen (1980), based on a beach ridge near the mouth of Pāuatahanui Inlet, and a ~ 1 m uplift estimate by Adkin (1921), based on wave-cut platform evidence west of the Ohariu Fault (Fig. 1). The ~30 cm minimum uplift estimate of Lyell (1856, in Grapes and Downes, 2010) appears to be an underestimate and is contradicted by much of the historical and sedimentological records. The extreme >2 m uplift estimate of Sheehan (1987), based on the fact that ships could no longer enter Te-Awarua-o-Porirua Harbour, is considered therefore to be an overestimate which can be attributed to the effects of siltation in the harbour following the earthquake, and subsequent rapid sedimentation associated with development around the inlet (Healy et al., 1980; Swales et al., 2005; Gibb and Cox, 2009; Stevens, 2017). Geomorphological evidence for 1855 uplift east of the Ohariu fault, such as the beach ridge reported by McFadgen (1980) which is no longer prominent, may be obscured by the coastal road and footpath around the edge of the inlet.

5.2. Post-1855 sea level change and implications for VLM in the Wellington region

Applying the age model from Fig. 7b to the reconstruction from PauM1 (Fig. 6) enables the relative sea-level rise at Pāuatahanui to be compared with that at Wellington tide gauge, which spans from 1901 to

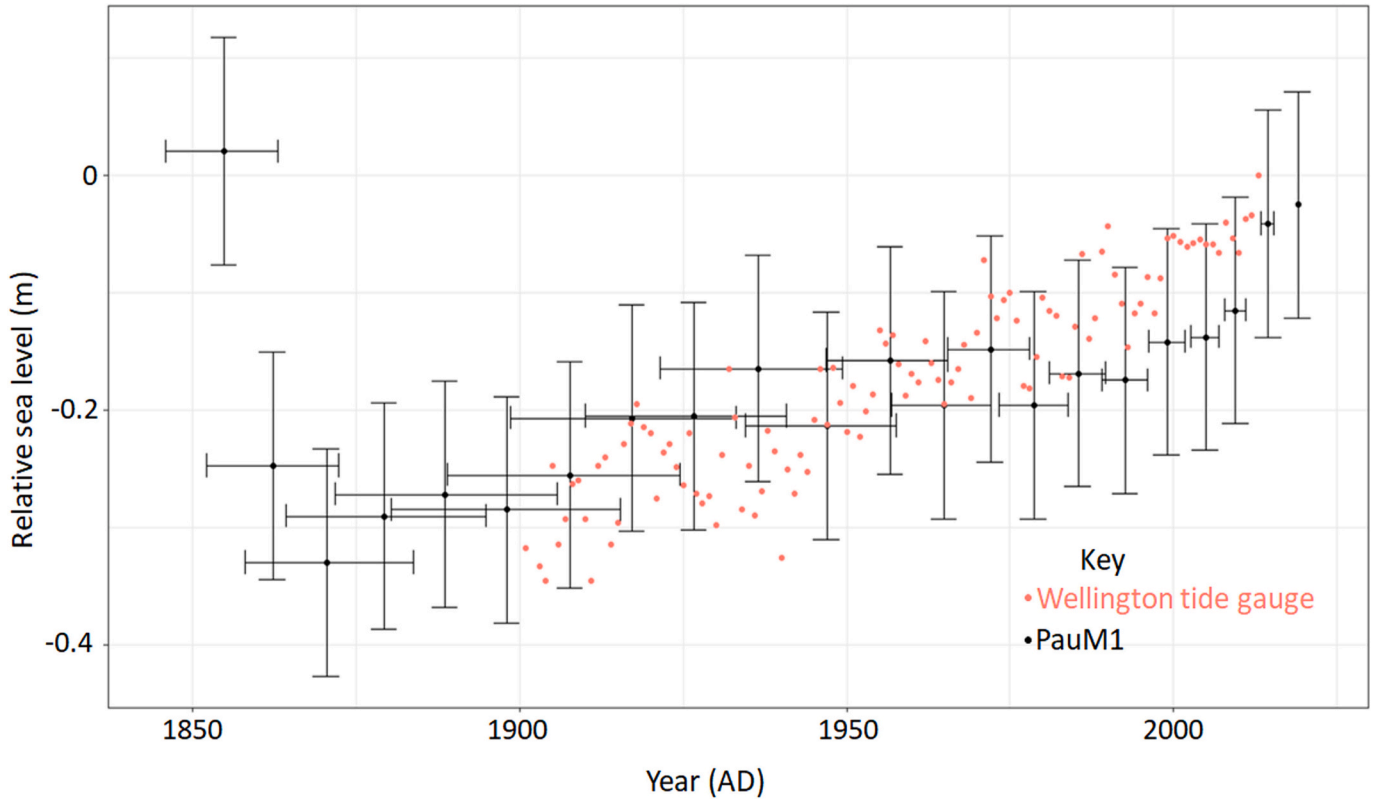

Fig. 9. Sea-level reconstruction from Pāuatahanui (PauM1), from the 1855 earthquake until present, plotted alongside the Wellington tide gauge. Sample age error bars are to a 95% confidence interval, while sea-level error bars are based on the RMSEP of the transfer function model.

2013 (Ministry for the Environment, 2021) (Fig. 9). The Wellington tide gauge data almost entirely lies within error of the foraminiferal sea-level reconstruction. From the 20 cm-depth horizon (here taken to represent the approximate relative sea level at 1855 CE after sediments ceased to contain a mixed marsh/mudflat foraminiferal assemblage) to core top (2019) the average rate of relative sea-level rise is 1.5 ± 0.6 mm/yr, increasing from 1.0 ± 1.9 mm/yr (1855–1900) to 2.4 ± 0.8 mm/yr from 1900 to 2019).

Through analysis of the trends exhibited in the foraminiferal sea-level reconstruction, and comparison with the Wellington tide gauge, it is possible to gain an understanding of the processes that have influenced relative sea level across the Wellington region since 1900, and extend these back to 1855 at Pāuatahanui. Our relative sea level reconstruction for 1855–1900 exceeds the climate-driven global mean sea level (GMSL) for this period (estimated at 0.4 ± 0.2 mm/yr, or 18 ± 9 mm (Walker et al., 2022) by ~0.6 mm/yr. Given the tectonic setting and observed regional subsidence in the instrumental era, we suggest that the difference indicates the average subsidence rate over this interval. However, due to the low model precision, the true subsidence rate may have been faster or slower. Furthermore, rates of 2.4 ± 0.8 mm/yr are derived from 1900 – present in this reconstruction. This exceeds the ~1.1 ± 0.3 mm/yr sea-level rise expected around New Zealand's coast during this interval (Tenzer and Gladkikh, 2014), indicating that subsidence on the order of ~1.3 mm/yr may be present across the twentieth century.

Whilst, these estimated rates of longer term subsidence are lower on average than most recently observed VLM rates in the region, we point out that when the full error range of our sea level reconstruction is considered, rates of up to 3.2 mm/yr sea-level rise are possible from Pāuatahanui across the twentieth and early twenty-first centuries. This upper estimate is consistent with the expected ~1.1 ± 0.3 mm/yr rate of relative sea-level rise around New Zealand excluding VLM (Tenzer and Gladkikh, 2014) plus −2.2 mm/yr VLM as indicated from InSAR (NZ SeaRise, 2022) or − 2.18 ± 0.17 mm/yr VLM (Tenzer and Fadil, 2016; Denys et al., 2020) as indicated from GNSS.

Our CPLR analysis indicates an apparent acceleration in sea level rise at Pāuatahanui from the 1990s-present (Supplementary Figs. 2–3). This feature may reflect either a recent initiation of modern VLM trends, or be the local expression of the globally documented acceleration in relative sea-level rise, which also accelerated to >3 mm/yr since this time (e.g. Dangendorf et al., 2017; Frederikse et al., 2020; Fox-Kemper et al., 2021). Indeed, a separate analysis of Wellington tide gauge data has argued that a continuous acceleration in the rate of relative sea-level rise is documented across its entire duration of measurements, from 1.23 ± 0.26 mm/yr from 1901 to 1960 to 2.84 ± 0.18 mm/yr from 1960 to 2020 (Stats NZ, 2022).

6. Conclusions

A new salt-marsh foraminiferal record at Pāuatahanui Inlet gives locally significant new insights into the impacts of the 1855 Mw 8.2 Wairarapa earthquake and subsequent relative sea level change through to the present day. Integrated lithologic and fossil data indicate the abrupt transition from a mudflat to upper salt marsh environment in agreement with the historical observations of the timing of the marsh formation. Transfer function outputs indicate that ~1 ± 0.45 m of sudden uplift occurred during the earthquake, supporting some previous estimates and contrary to other interpretations that no uplift occurred in the Porirua region at this time.

Following the establishment of the marsh, sea level has risen at a mean rate of 1.5 ± 0.6 mm/yr. The rate of relative sea level rise at the site has progressively increased from the 19th century (post-1855) (1.0 ± 1.9 mm/yr) to 2.4 ± 0.8 mm/yr during the twentieth century and > 3 mm/yr for the 21st century to date. This acceleration is consistent with trends in climate-driven global mean sea level over these periods, but the amounts of sea level rise consistently exceed GMSL rise, pointing to sustained net subsidence. The saltmarsh record lies entirely within error of the trend documented by the Wellington tide gauge, implying broad-scale applicability to the region. Whilst the mean SLR rates are higher than would be expected without subsidence, they are lower than would be expected on the basis of modern observations of adjacent subsidence (cf. Tenzer and Fadil, 2016; Bell et al., 2018; Levy et al., 2020; Hamling et al., 2022; NZ SeaRise, 2022). Those differences can be reconciled however when the full error range of the sea level reconstruction is considered. Although the precise impacts of VLM on the overall trend and its apparent rate changes cannot unambiguously be elucidated, this record shows that sustained subsidence should be factored into projections of future sea level for the region and its consequences.

This study demonstrates the capacity for salt marshes to produce robust sea-level reconstructions from tectonically unstable regions that can be useful for understanding impacts of local-regional relative sea level change in the future. In particular, saltmarsh sea-level reconstructions can reveal site-specific insights into the role of vertical land movement in recent decades to centuries, providing greater confidence in future sea level projections at these timescales.

Supplementary data to this article can be found online at https://doi.org/10.1016/j.margeo.2023.107199.

CRediT authorship contribution statement

Daniel J. King: Conceptualization, Data curation, Formal analysis, Investigation, Methodology, Writing – original draft. **Rewi M. Newnham:** Conceptualization, Formal analysis, Funding acquisition, Investigation, Methodology, Project administration, Resources, Supervision, Writing – original draft, Writing – review & editing. **Andrew B.H. Rees:** Methodology, Software. **Kate J. Clark:** Conceptualization, Investigation, Methodology, Resources, Supervision. **Ed Garrett:** Conceptualization, Formal analysis, Investigation, Methodology, Supervision. **W. Roland Gehrels:** Conceptualization, Investigation, Methodology, Project administration, Resources, Supervision. **Timothy R. Naish:** Conceptualization, Funding acquisition. **Richard H. Levy:** Conceptualization, Funding acquisition.

Declaration of Competing Interest

The authors declare that they have no known competing financial interests or personal relationships that could have appeared to influence the work reported in this paper.

Data availability

The data presented in this work are available at: https://doi.org/10.6084/m9.figshare.23618931.v1

Acknowledgements

Katharina Hecht (Utrecht University/Victoria University of Wellington), Jiten Patel (Victoria University of Wellington), Charlotte Pizer (Victoria University of Wellington) and Garth Archibald (GNS Science) are thanked for their invaluable assistance in fieldwork and surveying. Dr. Michael Lechermann (ESR Christchurch) and Dr. Levi Bourke (ESR Christchurch) are thanked for the generation of ^{210}Pb data, and Dr. Maarten Blaauw (Queen's University, Belfast) and Adelaine Moody (Victoria University of Wellington) are thanked for their assistance in the generation of ^{210}Pb age models. Dr. Valerie van den Bos (Victoria University of Wellington) is thanked for her work preparing our pollen samples for analysis, and her help with coding issues. Dr. Sophie Williams is also thanked for her useful discussions and further help with coding issues. Dez Tessler is also thanked for help with issues affecting the RTK GPS device during fieldwork. We also thank Marianna Terezow (GNS Science), Dr. Martin Crundwell (GNS Science), and Dr. Richard Pearce (National Oceanography Centre, Southampton) for their

help with scanning electron microscopy, used to generate the micrographs presented in Fig. 2. Rohini Biradavolu (Victoria University of Wellington) and the staff of Arapaki Manners Library are thanked for their assistance in finding difficult-to-access literature. Furthermore, Dr. Bruce Hayward is thanked for his invaluable discussions and opinions over the course of this project.

This project was funded by and is a contribution to the NZ SeaRise Project, an MBIE (Ministry of Business, Innovation and Employment)-funded program. Data are available at: httphttps://doi.org/10.6084/m9.figshare.23618931

References

Adkin, L., 1917. General view of the sale-yards. In: The Pahautanui cattle fair, Nov. 9. 1917'. From the album: Family photograph album; 1917–1920. https://collections.tepapa.govt.nz/object/905298 (accessed 18 October 2021).

Adkin, G.L., 1921. Porirua Harbour: a study of its shore-line and other physiographic features. Trans. Proc. of the R. Soc. N. Z. 53, 144–156.

Andersen, T.J., 2017. Some practical considerations regarding the application of 210Pb and 137Cs dating to estuarine sediments. In: Weckström, K., Saunders, K.M., Gell, P. A., Skillbeck, C.G. (Eds.), Applications of Paleoenvironmental Techniques in Estuarine Studies. Springer Nature, Dordrecht, pp. 121–140.

Appleby, P.G., 1998. Dating Recent Sediments by 210Pb: Problems and Solutions. University of Liverpool, Liverpool.

Aquino-López, M.A., Blaauw, M., Christen, J.A., Sanderson, N.K., 2018. Bayesian analysis of ^{210}Pb dating. J. Agric. Biol. Environ. Stat. 23 (3), 317–333. https://doi.org/10.1007/s13253-018-0328-7.

Barbosa, C.F., Scott, D.B., 2006. Emendation of the genus Trochammina Parker and Jones for improvement of work in the paralic environments. Anu. Inst. Geocienc. 29, 403–404. https://doi.org/10.11137/2006_1_401-404.

Barlow, N.L.M., Shennan, I., Long, A.J., Gehrels, W.R., Saher, M.H., Woodroffe, S.A., Hillier, C., 2013. Salt marshes as late Holocene tide gauges. Glob. Planet. Chang. 106, 90–110. https://doi.org/10.1016/j.gloplacha.2013.03.003.

Beavan, R.J., Litchfield, N.J., 2012. Vertical Land Movement Around the New Zealand Coastline: Implications for Sea-Level Rise. GNS Science Ltd., Lower Hutt. 2012/29.

Bell, R., 2021. How will our coasts and estuaries change with sea-level rise? Implications for communities and infrastructure. In: Clark, H. (Ed.), Climate Aotearoa: What's Happening & What Can we Do about it? Allen & Unwin, Auckland, pp. 62–92.

Bell, R.G., Denys, P., Hannah, J., 2018. Update on relative sea-level rise and vertical land motion: Wellington region. National Institute of Water & Atmospheric Research Ltd., Hamilton, 2019007HN.

Bellingham, N., 1998. Land, Sea and People: Geological and Historical Background. Pauatahanui Inlet - A Living Resource, Guardians of Pauatahanui Inlet, Pauatahanui.

Bennett, W.C., 1858. The New Zealand Earthquake. Rep. Br. Assoc. Adv. Sci. 28, 105–106.

Bernhard, J.M., Ostermann, D.R., Williams, D.S., Blanks, J.K., 2006. Comparison of two methods to identify live benthic foraminifera: a test between Rose Bengal and CellTracker Green with implications for stable isotope paleoreconstructions. Paleoceanogr. 21 (4), PA4210 https://doi.org/10.1029/2006PA001290.

Biggs, J., Wright, T.J., 2020. How satellite InSAR has grown from opportunistic science to routine monitoring over the last decade. Nat. Commun. 11 (1), 1–4. https://doi.org/10.1038/s41467-020-17587-6.

Bird, E.C.F., 1996. Coastal Erosion and rising Sea Level. In: Milliman, J.D., Haq, B.U. (Eds.), Sea-Level Rise and Coastal Subsidence: Causes, Consequences, and Strategies. Springer Science + Business Media, Dordrecht, pp. 87–103.

Birks, H.J.B., 1995. Quantitative palaeoenvironmental reconstructions. In: Maddy, D., Brew, J.S. (Eds.), Statistical Modelling of Quaternary Science Data. Quaternary Research Association, Cambridge, pp. 161–254.

Birks, H.J.B., 1998. Numerical tools in palaeolimnology - Progress, potentialities, and problems. J. Paleolomnol. 20, 307–332.

Blaauw, M., Christen, J.A., Aquino-Lopez, M.A., Esquivel-Vazquez, J., Gonzalez, O.M., Belding, T., Theiler, J., Gough, B., Karney, C., 2021. rplum: Bayesian Age-Depth Modelling of Cores Dated by Pb-210. https://cran.r-project.org/web/packages/rplum/index.html (accessed 5 November 2021).

Blaschke, P., Woods, J., Forsyth, F., 2010. The Porirua Harbour and its Catchment: A Literature Summary and Review Report for Porirua City Council & Wellington City Council. Blaschke and Rutherford Environmental Consultants, Wellington.

Bruel, R., Sabatier, P., 2020. serac: an R package for ShortlivEd RAdionuclide chronology of recent sediment cores. J. Environ. Radioact. 225, 106449 https://doi.org/10.1016/j.jenvrad.2020.106449.

Brünnich, M.T., 1772. Zoologiae Fundamenta. The author, Copenhagen.

Cahill, N., 2021. Bayesian Change-Point Linear Regression. https://www.niamhcahill.com/post/cptutorial/.

Cahill, N., Rahmstorf, S., Parnell, A.C., 2015. Change points of global temperature. Environ. Res. Lett. 10, 084002 https://doi.org/10.1088/1748-9326/10/8/084002.

Callard, S.L., Gehrels, W.R., Morrison, B.V., Grenfell, H.R., 2011. Suitability of salt-marsh foraminifera as proxy indicators of sea level in Tasmania. Mar. Micropaleontol. 79 (3), 121–131. https://doi.org/10.1016/j.marmicro.2011.03.001.

Camacho, S.G., Moura, D.M.D.J., Connor, S., Scott, D.B., Boski, T., 2015. Taxonomy, ecology and biogeographical trends of dominant benthic foraminifera species from an Atlantic-Mediterranean estuary (the Guadiana, southeast Portugal). Palaeontol. Electron. 18 (1), 17A.

Carlin, B.P., Gelfand, A.E., Smith, A.F.M., 1992. Hierarchical Bayesian analysis of changepoint problems. J. R. Stat. Soc.: Ser. C: Appl. Stat. 41 (2), 389–405. https://doi.org/10.2307/2347570.

Chen, H., Shaw, T.A., Wang, J., Engelhart, S., Nikitina, D., Pilarcsyk, J.E., Walker, J., García-Artola, A., Horton, B.P., 2020. Salt-Marsh Foraminiferal Distributions from Mainland Northern Georgia, USA: an assessment of their viability for sea-level studies. Open. Quat. 6 (6), 1–19. https://doi.org/10.5334/oq.91.

Clark, K.J., Hayward, B.W., Cochran, U.A., Grenfell, H.R., Hemphill-Haley, E., Mildenhall, D.C., Hemphill-Haley, M.A., Wallace, L.M., 2011. Investigating subduction earthquake geology along the southern Hikurangi margin using palaeoenvironmental histories of intertidal inlets. N. Z. J. Geol. Geophys. 54 (3), 255–271. https://doi.org/10.1080/00288306.2011.562903.

Clark, K., Howarth, J., Litchfield, N., Cochran, U., Turnbull, J., Dowling, L., et al., 2019. Geological evidence for past large earthquakes and tsunamis along the Hikurangi subduction margin, New Zealand. Mar. Geol. 412, 139–172. https://doi.org/10.1016/j. margeo.2019.03.004.

Clement, A.J.H., Whitehouse, P.L., Sloss, C.R., 2016. An examination of spatial variability in the timing and magnitude of Holocene relative sea-level changes in the New Zealand archipelago. Quat. Sci. Rev. 113, 73–101. https://doi.org/10.1016/j.quascirev.2015.09.025.

Conwell, R., 2010. Pauatahanui Wildlife Reserve - the First 25 Years. Nature Space, Wellington.

Cook, N.J., Ehrig, K.J., Rollog, M., Ciobanu, C.L., Lane, D.J., Schmandt, D.S., Owen, N.D., Hamilton, T., Grano, S.R., 2018. 210Pb and 210Po in geological and related anthropogenic materials: implications for their mineralogical distribution in base metal ores. Miner. 8, 211. https://doi.org/10.3390/min8050211.

Corbett, D.R., Walsh, J.P., 2015. 210Lead and 137Cesium: establishing a chronology for the last century. In: Shennan, I., Long, A.J., Horton, B.P. (Eds.), Handbook of Sea-Level Research. John Wiley & Sons, Ltd., Hoboken, pp. 361–372. https://doi.org/10.1002/9781118452547.ch24.

Crum, N.J., Neyman, L.C., Gowan, T.A., 2021. Abundance estimation for line transect sampling: a comparison of distance sampling and spatial capture-recapture models. PLoS One 16 (5). https://doi.org/10.1371/journal.pone.0252231 e0252231.

Cushman, J.A., Bronnimann, P., 1948a. Additional new species of arenaceous foraminifera from shallow waters of Trinidad. Contrib. Cushman Found. Foraminifer. Res. 24, 37–42.

Cushman, J.A., Bronnimann, P., 1948b. Some new genera and species of foraminifera from brackish water of Trinidad. Contrib. Cushman Found. Foraminifer. Res. 24, 15–21.

Dangendorf, S., Marcos, M., Wöppelmann, G., Conrad, C.P., Frederikse, T., Riva, R., 2017. Reassessnment of 20th century global mean sea level rise. Proc. Natl. Acad. Sci. U S A, p. 201616007.

Denys, P.H., Beavan, R.J., Hannah, J., Pearson, C.F., Palmer, N., Denham, M., Hreinsdottir, S., 2020. Sea level rise in New Zealand: the effect of vertical land motion on century-long tide gauge records in a tectonically active region. J. Geophys. Res. Solid Earth 125 (1). https://doi.org/10.1029/2019JB018055 e2019JB018055.

Downes, G.L., 2005. The 1855 January 23 M8+ Wairarapa earthquake - what contemporary accounts tell us about it. In: Townend, J., Langridge, Jones, A. (Eds.), The 1855 Earthquake Symposium. Greater Wellington Regional Council, Wellington, pp. 1–10.

Drexler, J.Z., Fuller, C.C., Archfield, S., 2018. The approaching obsolescence of 137Cs dating of wetland soils in North America. Quat. Sci. Rev. 199, 83–96. https://doi.org/10.1016/j.quascirev.2018.08.028.

Eggermont, H., Heiri, O., Verschuren, D., 2006. Fossil Chironomidae (Insecta: Diptera) as quantitative indicators of past salinity in African lakes. Quat. Sci. Rev. 25 (15), 1966–1994. https://doi.org/10.1016/j.quascirev.2005.04.011.

Eiby, G., 1990. Changes to Porirua Harbour in about 1855 : historical tradition and geological evidence. J. R. Soc. N. Z. 20 (2), 233–248. https://doi.org/10.1080/03036758.1990.10426727.

Erkens, G., Bucx, T., Dam, R., de Lange, G., Lambert, J., 2015. Sinking coastal cities. Proc. Intern. Assoc. Hydrol. Sci. 372, 189–198. https://doi.org/10.5194/piahs-372-189-2015.

Fedaeff, N., Fauchereau, N., 2015. Relationship between Climate Modes and Hawke's Bay Seasonal Rainfall and Temperature. National Institute of Water & Atmospheric Research Ltd., Auckland (KL2015-016).

Fisher, S., 2016. New Zealand's Alpine Fault biggest mover in the world. https://blogs.agu.org/geospace/2016/03/08/new-zealands-alpine-fault-biggest-mover-in-the-world/.

Forest and Bird Pāuatahanui Reserve Committee, 2009. Development time line for Pauatahanui Wildlife Reserve. https://web.archive.org/web/20210220224543/https://www.naturespace.org.nz/sites/default/files/Timeline_V_3_0.pdf (accessed 14 April 2020).

Fox-Kemper, B., Hewitt, H.T., Xiao, C., Aðalgeirsdóttir, G., Drijfhout, S.S., Edwards, T.L., Golledge, N.R., Hemer, M., Kopp, R.E., Krinner, G., Mix, A., Notz, D., Nowicki, S., Nurhati, I.S., Ruiz, L., Sallée, J.-B., Slangen, A.B.A., Yu, Y., 2021. Ocean, cryosphere and sea level change. In: Masson-Delmotte, V., Zhai, P., Pirani, A., Connors, S.L., Péan, C., Berger, S., Caud, N., Chen, Y., Goldfarb, L., Gomis, M.I., Huang, M., Leitzell, K., Lonnoy, E., Matthews, J.B.R., Maycock, T.K., Waterfield, T., Yelekçi, O., Yu, R., Zhou, B. (Eds.), Climate Change 2021: The Physical Science Basis. Contribution of Working Group I to the Sixth Assessment Report of the Intergovernmental Panel on Climate Change. Cambridge University Press, Cambridge, pp. 1211–1362.

Frail-Gauthier, J.L., Mudie, P.J., Simpson, A.G.B., Scott, D.B., 2019. Mesocosm and microcosm experiments on the feeding of temperate salt marsh foraminifera. J. Foraminifer. Res. 49 (3), 259–274. https://doi.org/10.2113/gsjfr.49.3.259.

Frederikse, T., Landerer, F., Caron, L., Adhikari, S., Parkes, D., Humphrey, V.W., Dangendorf, S., Hogarth, P., Zanna, L., Cheng, L., Wu, Y.-H., 2020. The causes of sea-level rise since 1900. Nat. 584 (7821), 393–397.
Garrett, E., Gehrels, W.R., Hayward, B.W., Newnham, Gehrels, M.J., Morey, C.J., Dangendorf, S., 2022. Drivers of 20th century sea-level change in southern New Zealand determined from proxy instrumental records. J. Quat. Sci. 37 (6), 1025–1043.
Gehrels, W.R., 1994. Determining relative sea-level change from salt-marsh Foraminifera and plant zones on the Coast of Maine, U.S.A. J.Coast. Res. 10 (4), 990–1009.
Gehrels, W.R., Belknap, D.F., 1993. Neotectonic history of eastern Maine evaluated from historic sea-level data and 14C dates on salt-marsh peats. Geol. 21 (7), 615–618.
Gehrels, W.R., Kemp, A.C., 2021. Salt marsh sediments as recorders of holocene relative sea-level change. In: FitzGerald, D.M., Hughes, Z.J. (Eds.), Salt Marshes: Function, Dynamics and Stresses. Cambridge University Press, Cambridge, pp. 225–256. https://doi.org/10.1017/9781316888933.011.
Gehrels, W.R., van de Plassche, O., 1999. The use of Jadammina macrescens (Brady) and Balticammina pseudomacrescens Brönnimann, Lutze and Whittaker (Protozoa: Foraminiferida) as sea-level indicators. Palaeogeogr. Palaeoclimatol. Palaeoecol. 149 (1), 89–101. https://doi.org/10.1016/S0031-0182(98)00194-1.
Gehrels, W.R., Hayward, B.W., Newnham, R.M., Southall, K.E., 2008. A 20th century acceleration of sea-level rise in New Zealand. Geophys. Res. Lett. 35 (2), L02717.
GeoNet, 2020. PAEK (Paekakariki Hill) – displacement from initial position. https://fits.geonet.org.nz/plot?siteID=PAEK&typeID=u&days=8000 (accessed 5 May 2020).
GeoNet, 2021a. PAEK - Look up observations. http://fits.geonet.org.nz/observation?typeID=u&siteID=PAEK (accessed 23 November 2021).
GeoNet, 2021b. WGTT - Look up observations. http://fits.geonet.org.nz/observation?typeID=u&siteID=WGTT (accessed 23 November 2021).
GeoNet, 2021c. TRWH - Look up observations. http://fits.geonet.org.nz/observation?typeID=u&siteID=TRWH (accessed 30 November 2021).
GeoNet, 2021d. KAPT - Look up observations. http://fits.geonet.org.nz/observation?typeID=u&siteID=KAPT (accessed 23 November 2021).
Giba, M., Walsh, J.J., Nicol, A., Mouslopoulou, V., 2013. Investigation of the spatio-temporal relationship between normal faulting and arc volcanism on million-year time scales. J. Geol. Soc. Lond. 170, 951–962. https://doi.org/10.1144/jgs2012-121.
Gibb, J.G., 2012. Local Relative Holocene sea-level changes for the Porirua Harbour area, Greater Wellington region. Coastal Management Consultancy Ltd., Kerikeri. CR 2012/1.
Gibb, J.G., Cox, G.J., 2009. Patterns and rates of sedimentation within Porirua Harbour, Kerikeri. Coastal Management Consultancy Ltd., Kerikeri. C.R.2009/1.
Grapes, R., Downes, G., 1997. The 1855 Wairarapa, New Zealand, earthquake - analysis of the historical data. Bull. N. Z. Natl. Soc. Earthq. Eng. 40 (4), 273–367. https://doi.org/10.5459/bnzsee.30.4.271-368.
Grapes, R.H., Downes, G.L., 2010. Charles Lyell and the great 1855 earthquake in New Zealand: first recognition of active fault tectonics. J. Geol. Soc. Lond. 167 (1), 35–47. https://doi.org/10.1144/0016-76492009-104.
Guardians of Pāuatahanui Inlet, 2021. Where and what is the reserve? https://www.gopi.org.nz/the-inlet/natural-history/wildlife-reserve/ (accessed 22 October 2021).
Hamling, I.J., Wright, T.J., Hreinsdóttir, S., Wallace, L.M., 2022. A snapshot of New Zealand's dynamic deformation field from envisat InSAR and GNSS observations between 2003 and 2011. Geophys. Res. Lett. 49 (2) https://doi.org/10.1029/2021GL096465 e2021GL096465.
Hannah, J., Bell, R.G., 2020. Forensic analysis of the 1944 datum shift at the Wellington tide gauge. N. Z. Surv. 306, 1–20.
Hayward, B.W., Grenfell, H.R., Scott, D.B., 1999a. Tidal range of marsh foraminifera for determining former sea-level heights in New Zealand. N. Z. J. Geol. Geophys. 42 (3), 395–413. https://doi.org/10.1080/00288306.1999.9514853.
Hayward, B.W., Grenfell, H.R., Reid, C.M., Hayward, K.A., 1999b. Recent New Zealand Shallow Water Benthic Foraminifera: Taxonomy, Ecologic Distribution, Biogeography, and Use in Paleoenvironmental Assessment. GNS Science Ltd., Lower Hutt.
Hayward, B.W., Grenfell, H.R., Kay, J., Sabaa, A.T., 2008. Foraminiferal evidence for Holocene history of Pauatahanui Inlet. Geomarine Research, Auckland. BWH 115/08.
Hayward, B.W., Figueira, B.O., Sabaa, A.T., Buzas, M.A., 2014. Multi-year life spans of high salt marsh agglutinated foraminifera from New Zealand. Mar. Micropaleontol. 109, 54–65. https://doi.org/10.1016/j.marmicro.2014.03.002.
Hayward, B.W., Holzmann, M., Pawlowski, J., Parker, J.H., Kaushik, T., Toyofuku, M.S., Tsuchiya, M., 2021. Molecular and morphological taxonomy of living Ammonia and related taxa (Foraminifera) and their biogeography. Micropaleontol. 67 (2–3), 109–313. https://doi.org/10.47894/mpal.67.2-3.01.
Healy, W.B., Atkinson, I.A.E., Barker, P.R., Bewick, D., Brodie, J.W., Burns, D.A., Campbell, A., Coker, P.M., Curry, R.J., Downes, C.J., Estcourt, I.N., Forch, E., Grange, K.R., Grant-Taylor, T., Hayden, B.J., Heath, R.A., Hovey, C., Ingram, P.M., Irwin, J., Kennedy, P., McColl, R.H.S., McDougall, J.C., Mildenhall, D.C., Milne, D. G., Mines, A.N., Northey, R.D., Pickrill, R.A., Rawlence, D.J., Read, G.B., Richardson, J.R., Ridgway, N.M., Smith, A., Till, D.G., Turner, J.C., 1980. Pauatahanui Inlet - An Environmental Study. New Zealand Department of Scientific and Industrial Research, Wellington.
Hesemann, M., 2020a. *Reophax scorpiurus* de Montfort, p. 1808. http://www.foraminifera.eu/singleplum.php?no=1001537&aktion=suche (accessed 29 April 2020).
Hesemann, M., 2020b. Reophax sp. http://www.foraminifera.eu/singleplum.php?no=1001713&aktion=suche (accessed 29 April 2020).
Hesemann, M., 2020c. Reophax sp. http://www.foraminifera.eu/singleplum.php?no=1005844&aktion=suche (accessed 29 April 2020).
Horton, B.P., 1999. The distribution of contemporary intertidal foraminifera at Cowpen Marsh, Tees Estuary, UK: implications for studies of Holocene Sea-level changes. Palaeogeogr. Palaeoclimatol. Palaeoecol. 149 (1), 127–149. https://doi.org/10.1016/S0031-0182(98)00197-7.
Houlié, N., Stern, T.A., 2017. Vertical tectonics at an active continental margin. Earth Planet. Sci. Lett. 457, 292–301. https://doi.org/10.1016/j.epsl.2016.10.018.
Javaux, E.J., Scott, D.B., 2003. Illustration of modern benthic foraminifera from Bermuda and remarks on distribution in other subtropical/tropical areas. Palaeontol. Electron. 6 (4), 1–29.
Juggins, S., 2019. RIOJA: Analysis of Quaternary Science Data. https://cran.r-project.org/web/packages/rioja/index.html (accessed 5th May 2020).
Kemp, A.C., Telford, R.J., 2015. Transfer Functions. In: Shennan, I., Long, A.J., Horton, B.P. (Eds.), Handbook of Sea-Level Research. John Wiley & Sons Ltd, Hoboken, pp. 470–497. https://doi.org/10.1002/9781118452547.ch31.
Kemp, A.C., Wright, A.J., Cahill, N., 2020. Enough is enough, or more is more? Testing the influence of foraminiferal count size on reconstructions of paleo-marsh elevation. J. Foraminifer. Res. 50 (3), 266–278. https://doi.org/10.2113/gsjfr.50.3.266.
King, D.J., 2017. North Atlantic climate variability at the onset of the Middle Eocene Climatic Optimum (MECO). University of Southampton, Southampton.
King, D.J., 2021. A re-evaluation of the foraminiferal genus Trochamminita (Cushman and Brönnimann, 1948) in New Zealand and a description of Pseudotrochamminita malcolmi (new genus, new species). J. Foraminifer. Res. 51 (4), 308–317.
King, D.J., Newnham, R.M., Gehrels, W.R., Clark, K.J., 2020. Late Holocene Sea-level changes and vertical land movements in New Zealand. N. Z. J. Geol. Geophys. 64 (1), 21–36. https://doi.org/10.1080/00288306.2020.1761839.
Kopp, R.E., Horton, R.M., Little, C.M., Mitrovica, J.X., Oppenheimer, M., Rasmussen, D. J., Strauss, B.H., Tebali, C., 2014. Probabilistic 21st and 22nd century sea-level projections at a global network of tide-gauge sites. Earth's Future 2 (8), 383–406. https://doi.org/10.1002/2014EF000239.
Kopp, R.E., Horton, B.P., Kemp, A.C., Tebali, C., 2015. Past and future sea-level rise along the coast of North Carolina, USA. Clim. Chang. 132, 693–707. https://doi.org/10.1007/s10584-015-1451-x.
Kopp, R.E., DeConto, R.M., Bader, D.A., Hay, C.C., Horton, R.M., Kulp, S., Oppenheimer, M., Pollard, D., Strauss, B.H., 2017. Evolving understanding of Antarctic ice-sheet physics and ambiguity in probabilistic sea-level projections. Earth's Future 5, 1217–1233. https://doi.org/10.1002/2017EF000663.
Levy, R., Naish, T., Bell, R., Golledge, N., Clarke, L., Garner, G., Hamling, I., Heine, Z., Hreinsdottir, S., Lawrence, J., Lowry, D., Priestley, R., Vargo, L., 2020. Te tai pari o aotearoa - future sea level rise around New Zealand's dynamic coastline. N. Z. Coast. Soc. Special. Publ. 4, 11–20.
Li, Y., Zhou, L., Cui, H., 2008. Pollen indicators of human activity. Chin. Sci. Bull. 53, 1281–1293. https://doi.org/10.1007/s11434-008-0181-0.
Litchfield, N., Van Dissen, R., Heron, D., Rhoades, D., 2006. Constraints on the timing of the three most recent surface rupture events and recurrence interval for the Ohariu Fault: trenching results from MacKays Crossing, Wellington, New Zealand. N. Z. J. Geol. Geophys. 49, 57–61. https://doi.org/10.1080/00288306.2006.9515147.
Loáiciga, H.A., Pingel, T.J., Garcia, E.S., 2011. Sea water intrusion by sea-level rise: scenarios for the 21st Century. Groundw. 50 (1), 37–47. https://doi.org/10.1111/j.1745-6584.2011.00800.x.
Massey, A.C., Gehrels, W.R., Charman, D.J., White, S.V., 2006. An intertidal foraminifera-based transfer function for reconstructing Holocene Sea-level change in Southwest England. J. Foraminifer. Res. 36, 215–232. https://doi.org/10.2113/gsjfr.36.3.215.
McFadgen, B.G., 1980. Age relationship between a Maori plaggen soil and Moa-hunter sites on the West Wellington coast. N. Z. J. Geol. Geophys. 23 (2), 249–256. https://doi.org/10.1080/00288306.1980.10424210.
McFadgen, B., 2007. Hostile Shores: Catastrophic Events in Prehistoric New Zealand and their Impact on Maori Coastal Communities. Auckland University Press, Auckland.
McFadgen, B., 2010. Archaeoseismology - a New Zealand perspecitve. In: Otago School of Mines (Ed), A Salute to the Captain : Celebrating the 100th Birthday of Emeritus Professor J.B. Mackie. University of Otago, Dunedin, pp. 85–100.
McIsaacs, G., 2019a. History of New Zealand Speedways. https://www.historicspeedway.co.nz/NZ_Speedways.htm (accessed 21 April 2020).
McIsaacs, G., 2019b. Pauatahanui Speedway. https://www.historicspeedway.co.nz/pahautanuiPractice.htm (accessed 21 April 2020).
McManaway, T.D., Gaz, D., 1852. Pahauatahanui and Porirua - County Sheet No. 9, Paekakariki.
Mills, H., Kirby, J.R., Holgate, S.J., Plater, A.J., 2013. The distribution of contemporary Saltmarsh Foraminifera in a macrotidal estuary: an assessment of their viability for sea-level studies. J. Ecosyst. Ecography. 3 (3), 1–16. https://doi.org/10.4172/2157-7625.1000131.
Ministry for the Environment, 2021. Sea Level, Temperature, and Circulation Data. https://data.mfe.govt.nz/data/category/environmental-reporting/marine/sea-level-temperature-and-circulation/ (accessed 11th August 2021).
Montagu, G., 1808. Testacea Britannica, or Natural History of British Shells, Marine, Land, and Fresh-Water, Including the Most Minute. S. Woolmer, London.
Murray, J.W., 1991. Ecology and Palaeoecology of Benthic Foraminifera. Routledge, London.
Murray, J.W., 2000. The enigma of the continued use of total assemblages in ecological studies of benthic foraminifera. J. Foraminifer. Res. 30 (3), 244–245. https://doi.org/10.2113/0300244.
Naish, T., Levy, R., Hamling, I., Garner, G., Herinsdottir, S., Kopp, R., Golledge, N., Bell, R., Paulik, R., Lawrence, J., Denys, P., Gillies, T., Bengston, S., Clark, K., King, D., Litchfield, N., Newnham, R., Wallace, L., 2022. Working paper: the significance of vertical land movements at convergent plate boundaries in 2 probabilistic sea-level projections for AR6 scenarios: the New Zealand case. https:

//www.searise.nz/blog/2022/7/8/working-paper-the-significance-of-vertical-land-movements-at-convergent-plate-boundaries-in-1-probabilistic-sea-level-projections-for-ar6-scenarios-the-new-zealand-case.
NatureSpace, 2009. Pauatahanui Chapel and Wetland in Background (1857). https://web.archive.org/web/20210220224501/https://www.naturespace.org.nz/sites/default/files/Pauatahanui_Chapel_and_wetland_in_background_1857.pdf (accessed 9 July 2020).
Nelson, A.R., Shennan, I., Long, A.J., 1996. Identifying coseismic subsidence in tidal-wetland stratigraphic sequences at the Cascadia subduction zone of western North America. J. Geophys. Res. Solid Earth 101 (B3), 6115–6135. https://doi.org/10.1029/95JB01051.
Newnham, R.M., Lowe, D.J., Wigley, G.N.A., 1995. Late Holocene palynology and palaeovegetation of tephra-bearing mires at Papamoa and Waihi Beach, western Bay of Plenty, North Island, New Zealand. J. R. Soc. N.Z. 25, 283–300. https://doi.org/10.1080/03014223.1995.9517490.
Nicholls, R.J., Lincke, D., Hinkel, J., Brown, S., Vafeidis, A.T., Meyssignac, B., Hanson, S. E., Merkens, J.-L., Fang, J., 2021. A global analysis of subsidence, relative sea-level change and coastal flood exposure. Nat. Clim. Chang. 11 (4), 338–342. https://doi.org/10.1038/s41558-021-00993-z.
Ninis, D., Howell, A., Little, T., Litchfield, N., 2023. Causes of permanent vertical deformation at subduction margins: evidence from late Pleistocene marine terraces of the southern Hikurangi margin Aotearoa New Zealand. Front. Earth Sci. 11 https://doi.org/10.3389/feart.2023.1028445.
NZ SeaRise, 2022. NZ SeaRise – Using the Map. https://searise.takiwa.co/map/6233f47872b8190018373db9/embed (accessed 11 May 2022).
Oksanen, J., Blanchett, F.G., Friendly, M., Kindt, R., Legende, P., McGlinn, D., Minchin, P.R., O'Hara, R.B., Simpson, G.L., Solymos, P., Stevens, M.H.H., Szoecs, E., Wagner, H., 2019. VEGAN: Community Ecology Package. CRAN R-Project. Ordination methods, diversity analysis and other functions for community and vegetation ecologists. A global analysis of subsidence, relative sea-level change and coastal flood exposure. https://cran.r-project.org/web/packages/vegan/vegan.pdf (accessed 17 September 2019).
Park, R., 1841. Map of the Village of Porirua with the Sacred Other Lots Adjoining. Wellington Survey Office, Wellington.
Plummer, M., Stukalov, A., Denwood, M., 2021. rjags: Bayesian Graphical Models using MCMC. https://cran.r-project.org/web/packages/rjags/index.html (accessed 6 April 2022).
Poitevin, C., Wöppelmann, G., Raucoules, D., Le Cozannet, G., Marcos, M., Testut, L., 2019. Vertical land motion and relative sea level changes along the coastline of Brest (France) from combined space-borne geodetic methods. Remote Sens. Environ. 222, 275–285. https://doi.org/10.1016/j.rse.2018.12.035.
R Core Team, 2022. R: A language and environment for statistical computing. https://www.R-project.org/ (Accessed 8 November 2022).
Reilly, H., 2013. Pāuatahanui: A Local History. Pāuatahanui Residents Association, Pāuatahanui.
Restrepo-Ángel, J.D., Mora-Páez, H., Díaz, F., Govorcin, M., Wdowinski, S., Giraldo-Londoño, L., Tosic, M., Fernández, I., Paniagua-Arroyave, J.F., Duque-Trujillo, J.F., 2021. Coastal subsidence increases vulnerability to sea level rise over twenty first century in Cartagena, Caribbean Colombia. Sci. Rep. 11, 18873. https://doi.org/10.1038/s41598-021-98428-4.
Retrolens, 2021. Historical Imagery Resource. https://retrolens.co.nz/map/#/1758033.5384139975/5446936.584756313/1762056.0370276107/5449425.565489914/2193/10 (accessed 27 October 2021).
Ryan, D., Clement, A.J.H., Jankowski, N.R., Stocchi, P., 2021. The last interglacial sea-level record of Aotearoa New Zealand. Earth. Syst. Sci. Data. 13 (7), 3399–3437. https://doi.org/10.5194/essd-13-3399-2021.
Sachs, H.M., Webb, T., Clark, D.R., 1977. Paleoecological transfer functions. Annu. Rev. Earth Planet. Sci. 5, 159–178. https://doi.org/10.1146/annurev.ea.05.050177.001111.
Saunders, J.B., 1957. Trochamminidae and certain Lituolidae (foraminifera) from the recent brackish-water sediments of Trinidad, British West Indies. Smithson. Misc. Collect. 134, 1–15.
Scott, D.B., 1976. Brackish-water foraminifera from southern California and description of Polysaccammina ipohalina n. gen., n. sp. J. Foraminifer. Res. 6 (4), 312–321. https://doi.org/10.2113/gsjfr.6.4.312.
Scott, D.B., Hermelin, O.R., 1993. A device for precision splitting of micropaleontological samples in liquid suspension. J. Paleontol. 67, 151–154. https://doi.org/10.1017/S0022336000021302.
Scott, D.B., Medioli, F.S., 1980. Quantitative studies of marsh foraminiferal distributions in Nova Scotia: implications for sea level studies. Cushman. Found. Foraminifer. Res. Special. Publ. 17, 4–59.
Scott, D.B., Medioli, F.S., 1986. Foraminifera as sea-level indicators. In: van de Plassche, O. (Ed.), Sea-Level Research. Geo Books, Norwich, pp. 435–456. https://doi.org/10.1007/978-94-009-4215-8_15.
Scott, D.B., Medioli, F.S., Schafer, C.T., 2001. Monitoring in Coastal Environments Using Foraminifera and Thecamoebian Indicators. Cambridge University Press, Cambridge.
Sheehan, M., 1987. An Introduction to the History of Porirua. Porirua Museum, Porirua.
Sheehan, M., 1988. Pauatahanui & The Inlet. Porirua History Series. Porirua Museum, Porirua.
Shennan, I., Garrett, E., Barlow, N., 2016. Detection limits of tidal-wetland sequences to identify variable rupture modes of megathrust earthquakes. Quat. Sci. Rev. 150, 1–30. https://doi.org/10.1016/j.quascirev.2016.08.003.
Shirzaei, M., Freymueller, J., Törnqvist, T.E., Galloway, D.L., Dura, T., Minderhoud, P.S. J., 2021. Measuring, modelling and projecting coastal land subsidence. Nat. Rev. Earth. Environ. 2, 40–58. https://doi.org/10.1038/s43017-020-00115-x.
Šmilauer, P., Lepš, J., 2014. Multivariate Analysis of Ecological Data Using CANOCO 5. Cambridge University Press, Cambridge.
Smith, S., 2010. Coastal Erosion & Sea Level rise. New South Wales Parliamentary Library, Sydney. 6/2010.
Southall, K.E., Gehrels, W.R., Hayward, B.W., 2006. Foraminifera in a New Zealand salt marsh and their suitability as sea-level indicators. Mar. Micropaleontol. 60 (2), 167–179. https://doi.org/10.1016/j.marmicro.2006.04.005.
Stats NZ, 2022. Coastal Sea-Level Rise. https://www.stats.govt.nz/indicators/coastal-sea-level-rise (accessed 26 April 2023).
Stephenson, G., 1986. Wetlands - Discovering New Zealand's Shy Places. Government Printing Office Publishing, Wellington.
Stevens, L.M., 2017. Porirua Harbour Sediment Plate Monitoring 2016/17. Wriggle Coastal Management Limited, Nelson.
Stone, M., 2021. Sinking land and rising seas: the dual crises facing coastal communities. https://www.nationalgeographic.com/environment/article/sinking-land-rising-seas-dual-crises-facing-coastal-communities (accessed 18 October 2021).
Su, Y.-S., Yajima, M., 2021. R2jags: Using R to Run 'JAGS'. https://cran.r-project.org/web/packages/R2jags/index.html.
Swales, A., Bentley, S.J., McGlone, M.S., Ovenden, R., Hermanspahn, N., Budd, R., Hill, A., Pickmere, S., Haskew, R., Okey, M.J., 2005. Pauatahanui Inlet: Effects of Historical Catchment Landcover Changes on Inlet Sedimentation. National Institute of Water & Atmospheric Research Ltd, Hamilton (HAM2004-149).
Swales, A., Bell, R., Lohrer, D., 2020. Estuaries and lowland brackish habitats. N. Z. Coast. Soc. Special. Publ. 4, 55–64.
Takherani, M., Viyousek, S., Barnard, P.L., Frazer, N., Anderson, T.R., Fletcher, C.H., 2020. Sea-level rise exponentially increases coastal flood frequency. Sci. Rep. 10, 6466. https://doi.org/10.1038/s41598-020-62188-4.
Telford, R.J., Birks, H.J.B., 2011. QSR Correspondence "is spatial autocorrelation introducing biases in the apparent accuracy of palaeoclimatic reconstructions?". Quat. Sci. Rev. 30 (21–22), 3210–3213. https://doi.org/10.1016/j.quascirev.2011.07.019.
Tenzer, R., Fadil, A., 2016. Tectonic classification of vertical crustal motions – a case study for New Zealand. Contrib. Geophys. Geodesy. 46 (2), 91–109. https://doi.org/10.1515/congeo-2016-0007.
Tenzer, R., Gladkikh, V., 2014. Analysis of the sea level change in New Zealand. In: Rizos, C., Willis, P. (Eds.), Earth on the Edge: Science for a Sustainable Future. Springer-Verlag, Berlin, pp. 135–139. https://doi.org/10.1007/978-3-642-37222-3_17.
ter Braak, C.J.F., Verdonschot, P.F.M., 1995. Canonical correspondence analysis and related multivariate methods in aquatic ecology. Aquat. Sci. 57 (3), 255–289. https://doi.org/10.1007/BF00877430.
Tobin, R., Scott, D.B., Collins, E.S., Medioli, F.S., 2005. Infaunal benthic foraminifera in some North American marshes and their influence on fossil assemblages. J. Foraminifer. Res. 35 (2), 130–147. https://doi.org/10.2113/35.2.130.
Troels-Smith, J., 1955. Karakterisering af lose jordater (Characterisation of Unconsolidated Sediments). Dan. Geol. Unders. 3, 39–73.
Walker, J.S., Cahill, N., Khan, N.S., Shaw, T.A., Barber, D., Miller, K.G., Kopp, R.E., Horton, B.P., 2020. Incorporating temporal and spatial variability of salt-marsh foraminifera into sea-level reconstructions. Mar. Geol. 429, 106293 https://doi.org/10.1016/j.margeo.2020.106293.
Walker, J.S., Kopp, R.E., Little, C.M., Horton, B.P., 2022. Timing of emergence of modern rates of sea-level rise by 1863. Nat. Commun. 13, 966. https://doi.org/10.1038/s41467-022-28564-6.
Wallace, L.M., 2020. Slow slip events in New Zealand. Annu. Rev. Earth Planet. Sci. 48 (1), 175–202. https://doi.org/10.1146/annurev-earth-071719-055104.
Wallace, L.M., Beavan, J., 2010. Diverse slow slip behavior at the Hikurangi subduction margin, New Zealand. J. Geophys. Res. Solid Earth 115 (B12), B12402. https://doi.org/10.1029/2010JB007717.
Wallace, L.M., Barnes, P., Beavan, J., Van Dissen, R.J., Litchfield, N.J., Mountjoy, J., et al., 2012. The kinematics of a transition from subduction to strike-slip: an example from the central New Zealand plate boundary. J. Geophys. Res. 117, B11402. https://doi.org/10.1029/2011JB008640.
Wickham, H., 2021. Tidyverse: Easily install and Load the "tidyverse". https://cran.r-project.org/web/packages/tidyverse/index.html (accessed 6 April 2022).
Williams, S., Garrett, E., Moss, P., Bartlett, R., Gehrels, R., 2021. Development of a Training Set of Contemporary Salt-Marsh Foraminifera for Late Holocene Sea- Level Reconstructions in southeastern Australia. Open Quat. 7 (1), 4. https://doi.org/10.5334/oq.93.
Williams, S.L., Garrett, E., Moss, P.T., Dangendorf, S., Hibbert, F.D.M., Atkinson, N.R., Pashley, V., Millar, I.L., Garnett, M.H., Zawadzki, A., Gehrels, W.R., 2023. Relative sea-level changes in southeastern Australia during the 19th and 20th centuries. J. Quat. Sci. https://doi.org/10.1002/jqs.3528.
Wilson, K., Cochran, U., 2008. It's Our Fault – Past Subduction Ruptures: Task Progress Report 2007-2008. GNS Science, Lower Hutt, 2008/173.
Wright, A.J., Edwards, R.J., van de Plassche, O., 2011. Reassessing transfer-function performance in sea-level reconstruction based on benthic salt-marsh foraminifera from the Atlantic coast of NE North America. Mar. Micropaleontol. 81 (1), 43–62. https://doi.org/10.1016/j.marmicro.2011.07.003.